NATIONAL AND KAPODISTRIAN UNIVERSITY OF ATHENS

SCHOOL OF POSITIVE SCIENCES
DEPARTMENT OF AEROSPACE SCIENCE AND TECHNOLOGY

Thesis

Detection of areas susceptible to land degradation in Mediterranean using remote sensed data and environmental quality indices

Sofia P. Karamani

Supervisor: Stavros Kolios, Assistant Professor

EVRIPOU COMPLEX

June 2024

Detection of areas susceptible to land degradation in Mediterranean using remote sensed data and environmental quality indices

Sofia P. Karamani

R.N. 1116202000038

Supervisor: Stavros Kolios, Assistant Professor

Contents

List of Figures

List of Tables

ABSTRACT

Land degradation in the Mediterranean region is a major environmental issue, caused by climate change, urbanization, human activity, and the depletion of water resources. Thus, its regions are particularly vulnerable to erosion, desertification, and biodiversity loss. Using remote sensing data and environmental quality indices, the area of interest is detected and monitored over the years using modern methods. Remote sensing includes high spatial resolution satellite data, using multispectral satellite image the environmental degradation of ecosystems. These technologies and methodologies provide valuable tools for decision-making and natural resource management, contributing to sustainable development and environmental protection. In the Mediterranean, land degradation is exacerbated by its climate (characterized by mild winters and hot, dry summers), its geomorphology (including mountain ranges, hilly areas, plains, and volcanic activity), and anthropogenic factors such as urbanization and agriculture.

ΠΕΡΙΛΗΨΗ

Η πτυχιακή εργασία αφορά τον εντοπισμό των περιοχών που είναι ευάλωτες στην υποβάθμιση του εδάφους της Μεσογείου με τη χρήση δεδομένων για τη χρονική περίοδο 2000 έως 2020. Τα δεδομένα που επιλέχθηκαν κατανεμήθηκαν σε 5 πίνακες που αντιπροσωπεύουν τους δείκτες ποιότητας, ανάλογα το είδος τους. Στον πίνακα 1 Δείκτης Ποιότητας Κλήματος, περιλαμβάνονται η βροχόπτωση και ο προσανατολισμό μιας τοποθεσίας σε σχέση με τις βασικές κατευθύνσεις (βοράς, νότος, ανατολή, δύση). Ο πίνακας 2 Δημογραφικός Δείκτης, αφορά την πυκνότητα του πληθυσμού και στον συνολικό αριθμό ατόμων που ζουν σε μια περιοχή. Στον Δείκτη Ποιότητας Εδάφους, έχουν χρησιμοποιηθεί τα δεδομένα για την μέση θερμοκρασία επιφάνειας εδάφους, την περιεκτικότητα υγρασίας εδάφους, την κλήση και την θερμοκρασία εδάφους (πίνακας 3). Για τον Δείκτη Ποιότητας Βλάστησης (πίνακας 4), επιλέχθηκαν η κάλυψη της γης και το ποσοστό βλάστησης. Τέλος για τον Δείκτη Ανταλλαγής Ενέργειας (πίνακας 5) αναγράφονται τα δεδομένα για το ποσοστό ηλιακής ακτινοβολίας που ανακλάται, την εξάτμιση και μεταφορά ενέργειας με τη μορφή λανθάνουσας θερμότητας μεταξύ της επιφάνειας της Γης και της ατμόσφαιρας. Στη συνέχεια, τα δεδομένα τροποποιήθηκαν, με σκοπό να καταλήξουν στην απαιτούμενη μορφή για τον τελικό υπολογισμό τους. Για τελικό υπολογισμό των δεικτών, αρχικά οριοθετήθηκε η περιοχή της Μεσογείου, με βάση τις συντεταγμένες 9.6662(W), 29.0247(N), 37.0573(E). Τα δεδομένα επεξεργάστηκαν, μετατρέποντας το μέγεθος των pixel σε 0,008x0,008 και δημιουργώντας κλάσεις (1,2,3,4), έτσι ώστε να είναι δυνατόν να πραγματοποιηθούν πράξεις μεταξύ τους. Οι τιμές των κλάσεων αντιπροσωπεύουν την ευαισθησία του εδάφους μιας περιοχής, δηλαδή η τιμή 1 δείχνει ότι η γεωγραφική περιοχή που καλύπτει αυτό το pixel είναι ανθεκτική και παρουσιάζεται με κόκκινο χρώμα, ενώ η τιμή 4 υποδηλώνει μεγάλη περιβαλλοντική ευαισθησία, που σημαίνει ότι το έδαφος έχει υποστεί υποβάθμιση. Έπειτα υπολογίστηκαν οι δείκτες ποιότητας του εδάφους, όπου ο καθένας αντιπροσωπεύεται από δεδομένα (πίνακες 1-5). Στη συνέχεια εκτιμήθηκε ο δείκτης των περιοχών με περιβαλλοντική ευαισθησία (ESAI), για όλη την χρονική περίοδο 2000-2020 αλλά και ανά πενταετία, ο οποίος προκύπτει από τους δείκτες ποιότητας (QI), παρέχοντας ένα ολοκληρωμένο πλαίσιο για τον προσδιορισμό των περιοχών που κινδυνεύουν από υποβάθμιση. Τέλος, η χωρική κατανομή των τιμών (ESAI) δείχνει ότι οι Ευρωπαϊκές χώρες έχουν αρκετά χαμηλότερες τιμές ESAI σε σύγκριση με της Βόρειας Αφρικής, γεγονός που δείχνει ότι η νότια Μεσόγειος είναι πιο ευάλωτη στην υποβάθμιση του εδάφους από ότι η βόρεια Μεσόγειος.

KEYWORDS

Mediterranean, environmental index, GIS, land degradation, remote sensed data

1. THEORETICAL BACKGROUND

1.1 Introduction

Land degradation represents a significant environmental challenge at the global level. The phenomenon is exacerbated by several factors, including climate change and extensive anthropogenic activities such as agriculture, urbanization, warming, arson, drought, water scarcity, and so forth. The combination of these factors gives rise to significant challenges, including the loss of vegetation, which renders the soil more susceptible to erosion by rainfall. This, in turn, impairs the capacity of the vulnerable region to undergo regeneration.

As stated by the International Panel on Climate Change (IPCC), a United Nations body established to assess the scientific aspects of climate change (2021), global climate change is not a future problem. The Earth's climate is already undergoing significant changes because of human-induced emissions of greenhouse gases, with widespread consequences for the environment. Glaciers and ice sheets are shrinking, river and lake ice is melting earlier, the geographic ranges of plants and animals are shifting, and trees are flowering earlier. The impacts scientists have long predicted would result from global climate change are now being observed, including the loss of sea ice, accelerated sea level rise and longer and more intense heat waves. The IPCC's Sixth Assessment Report, published in 2021, revealed that human emissions of heat trapping gases have already resulted in a warming of the clime by approximately 2 degrees Fahrenheit (1.1 degrees Celsius) since 1850-1900. It is anticipated that the global average temperature will reach or exceed 1.5 degrees Celsius (approximately 3 degrees Fahrenheit) over the coming decades. These changes will have an impact on all regions of the Earth[1].

A 2017 study by the United Nations Environment Programme (UNEP) revealed that the Mediterranean region is warming at a rate 20% faster than the global average. The Mediterranean region is home to over 510 million people. By 2050, it is anticipated that water demand will increase by a factor of two or even three. Global warming of 2°C is predicted to result in a reduction in rainfall of approximately 10 to 15%[2].

As stated in the book *Increased Anthropogenic Activity in the Mediterranean Since the Opening of the Suez Canal* by Palgrave Macmillan, (Cham, 2023), the total population of the Mediterranean countries grew from 276 million in 1970 to 412 million in 2000 (a 1.35% increase per year) and 466 million in 2010. The population is predicted to reach 529 million by 2025. The Mediterranean region's population is concentrated near the coast. More than a third live in coastal administrative entities totaling less than 12% of the surface area of the Mediterranean countries. The population of the coastal regions grew from 95 million in 1979 to 143 million in 2000. It could reach 174 million by 2025. The concentration of population in coastal zones is heaviest in the western Mediterranean, the western shore of the Adriatic Sea, the eastern shore of the Aegean-Levantine region, and the Nile Delta. Overall, the

[1] Bolles Dana, "The Effects of Climate Change" in *Climate Change*, NASA official web site, accessible by https://science.nasa.gov/climate-change/effects/ [Consulted 24/07/2024]

[2] Cherif Semia, [*et al.*], "Drivers of Change" in (Ed. Cramer W. *et al.) Climate and Environmental Change in the Mediterranean Basin. First Mediterranean Assessment Report (Mar 1),* Marseille, UNEP/MAP, 2020, p. 59-1034. DOI: 10.5281/zenodo.7224821 [Consulted 24/07/2024]

concentration of population in the coastal zone is higher in the southern Mediterranean countries. This is also where the variability of the population density in the coastal zone is highest, ranging from more than 1000 people/km^2 in the Nile Delta to fewer than 20 people/km^2 along parts of coastal Libya. Human activities, including shipping, invasive species, oil spills and others, have a direct impact on the Mediterranean Sea environment. This is evidenced by the direct impact of such activities on the marine environment, as well as the observed rise in ocean levels and the attendant biophysical changes in seawater[3].

The utilization of contemporary technology, encompassing the utilization of spatial data and satellite imagery at a spatial resolution of 0.1°-0.25°, corresponding to 11-28 km on the Earth's surface, enables the precise monitoring of environmental conditions and alterations in soil conditions. Consequently, substantial alterations in vegetation, erosion, soil moisture and other variables can be discerned, thereby facilitating precise and comprehensive assessment of extensive geological regions. This technology facilitates the monitoring and detection of environmental hazards, thereby assisting in the resolution of this phenomenon. The effects of climate change will increasingly worsen environmental degradation and disrupt socio-economic systems that rely on natural resources, leading to significant risks of population displacement. The most vulnerable nations, particularly least developed countries, will face consequences such as economic decline, flooding of coastal regions, and degradation of land and freshwater supplies[4].

The assessment and monitoring of the environment is conducted using Environmental Quality Indices, which combine a range of environmental parameters and data to provide comprehensive and quantitative assessment on a global scale. The parameters employed in this study are the Greenness Fraction Average Surface Skin Temperature, Soil Temperature, Soil Moisture Content, Evapotranspiration, Albedo, Latent Heat Net Flux, Precipitation Density, Precipitation Count and Precipitation. These parameters facilitate the identification of changes occurring every five years, thereby enabling the formulation of strategies to address environmental issues and conserve the natural resources of the Mediterranean.

The objective of this thesis is to identify areas within the Mediterranean region that are susceptible to land degradation, utilizing remote sensing data and environmental quality indicators. The Mediterranean region, with its distinctive climatic conditions, is one of the area's most severely affected by land degradation. The utilization of remote sensing data affords the opportunity to monitor extensive areas on a consistent and precise basis, which is pivotal for the responsible management of natural resources and the safeguarding of vulnerable regions. In this study, a variety of remote sensing data, including satellite imagery,

[3] Semion Polivon, "Increased Anthropogenic Activity in the Mediterranean Since the Opening of the Suez Canal", in (Ed. Lutmar C., Rubinovitz Z.) *The Suez Canal: Task Lessons and Features Challenges,* London*,* Palgrave Macmillan, January2023, p.217-229. DOI: https://doi.org/10.1007/978-3-031-15670-0_11 [Consulted 12/07/2024]

[4] Warner Koko, [*et al*], "Climate change, environmental degradation and migration", *Natural Hazards*, vol. 55, no 3, August 2009, p. 689-715. DOI: https://doi.org/10.1007/s11069-009-9419-7 [Consulted 3/07/2024]

will be utilized to evaluate soil condition and identify regions exhibiting a high risk of degradation. Environmental indicators will be employed to evaluate the degradation of Mediterranean soil from 2000 to 2020. Land degradation results in deforestation, desertification and soil erosion due to natural or man-made causes[5].

To conclude, the purpose of this study is to develop a comprehensive model for the identification of areas most vulnerable to degradation through the analysis of relevant data and indicators. This model may be used by stakeholders to undertake preventative measures and implement restoration strategies, thereby contributing to the management of the Mediterranean's natural resources.

QGIS is a public project hosted on QGIS.org, Licensed under the GNU GPLv2+, and owned by its contributors. It enables precise cartographic design and digitization. It is a comprehensive set off analysis tools that help to gain insight from the data provided. It is designed to create, process, analyze and visualize geospatial data. It also allows the processing of high-resolution maps. In this thesis, QGIS was used to process all the data. By downloading various existing maps, they were cropped according to the area of interest and then processed accordingly to the area of interest and then processed accordingly to create four classes which color code the sensitivity of each area, with each file having the same pixel size. QGIS then helped to produce the final indices by calculating the results of the Mediterranean maps and finding the differences in each period.

1.2 The Importance of Land Degradation

Land degradation is defined as the gradual reduction in the capacity of ecosystems to support biodiversity, agricultural production and water management. Particularly in the Mediterranean, drought conditions, combined with intensive agricultural exploitation and tourism development, have increased the vulnerability of areas causing degradation[6]. The UN Food and Agriculture Organization (FAO) considers land degradation to be one of the world's biggest environmental problems, affecting the ecological balance[7].

In regions such as the Mediterranean, where the environment is particularly vulnerable due to climatic and geomorphological specificity, the analysis and identification of vulnerable areas is important. Hot and dry climatic conditions, combined with heavy rainfall, lead to an increased risk of soil erosion. In addition, periods of drought affect the capacity of the soil to support vegetation, which increases the sensitivity of ecosystems causing erosion and degradation. At the same time, human activities have exacerbated this phenomenon. Agriculture, as well as deforestation, has contributed to a reduction in soil fertility. Tourism

[5] Kaiser Mohammad Shakil, "Land Degradation: Causes, Impacts, and Interlinks with the Sustainable Development Goals", in (Ed. Walter Leal Filho) *Encyclopedia of the UN Sustainable Development Goals*, Switzerland, Sprinter, 2021, p. 1-13. DOI: https://doi.org/10.1007/978-3-319-71062-4_48-1 [Consulted 20/06/2024]

[6] Magliulo Paolo, [*et al*.] "Changes in Land-Cover/Land-Use Pattern in the Fortore River Basin (Southern Italy) and Morphodynamic Implications", *Land*, vol. 12, no 7, 2023, p.13-93. DOI: https://doi.org/10.3390/land12071393 [Consulted 03/05/2024]

[7] FAO, "The State of the World's Forests", in *Forests, biodiversity and people,* Rome, FAO and UNEP, 2020, p. 1-214. DOI: https://doi.org/10.4060/ca8642en [Consulted 16/05/2024]

development in the Mediterranean coastal areas has also put pressure on the ecosystem, as it is often accompanied by the construction of infrastructure that disturbs the natural balance of the soil, biodiversity and hydrological function. Particularly in the southern Mediterranean regions, where biodiversity is already reduced and arable land is limited, land degradation has a devastating impact on food production and water management. Detecting and identifying areas at risk helps to better manage land to prevent erosion, biodiversity loss and desertification. The use of satellite data and environmental quality indicators helps to detect degradation early and develop preventive measures[8].

Through remote sensing, it is possible to obtain information on a large scale, both spatially and temporally. Remote sensing provides the ability to detect changes in land use, vegetation, soil moisture and other environmental parameters related to land degradation. The use of satellites offers important advantages, such as access to remote areas, continuous monitoring and the ability to analyze large geographical areas with precision.

1.3 The Role of Satellite Data

Through remote sensing, it is possible to obtain information on a large scale, both spatially and temporally. Remote sensing provides the ability to detect changes in land use, vegetation, soil moisture and other environmental parameters related to land degradation. The use of satellites offers important advantages, such as access to remote areas, continuous monitoring and the ability to analyze large geographical areas with precision.

Modern satellites such as Sentinel-2, Landsat 8 and 9, and MODIS have contributed to monitoring environmental changes related to land degradation. The European Space Agency's (ESA) Sentinel-2, through the Copernicus program, offers high spatial resolution images and is designed to monitor land and vegetation. MODIS (Moderate Resolution Imaging Spectroradiometer), installed on NASA's Terra and Aqua satellites, provides data on vegetation, temperature and humidity, contributing significantly to the detection of changes on Earth globally. Landsat 8 and 9 detect changes in land use. The GPM satellite provides accurate and continuous rainfall measurements on a global scale. GLDAS offers insights into land surfaces, including data on moisture, temperature and vegetation, through simulations and data from a range of satellites. The MERRA-2 satellite provides data on climate parameters such as temperature, precipitation and wind currents. The MERIS satellite provides bleaching and vegetation data. The use of these satellites provides information to monitor land degradation, facilitating the early detection of hazards and the development of protection and restoration strategies.

[8] Wulder Michael [*et al*.] "How free data has enabled the science and monitoring promise of Landsat. ", *Remote Sensing of Environment,* July/2012 vol. 122, p. 2-10. DOI: https://doi.org/10.1016/j.rse.2012.01.010 [Consulted 16/05/2024]

2. DATA COLLECTION AND METHODOLOGY

2.1 Area to be studied

The Mediterranean Sea is surrounded by a total of twenty-two countries (Figure 1), distributed across three continents. These include countries from Europe (France, Spain, Italy Monaco, Slovenia, Croatia, Bosnia and Herzegovina, Montenegro, Greece, Malta, Albania, and Spain), Asia (Syria, Lebanon, Turkey, Israel, the Gaza strip-Palestine and Cyprus) and Africa (Egypt, Libya, Tunisia, Algeria, Morocco). In the context of this thesis, the research concerns the geographical coordinates of the Mediterranean region: 9,6662°(W), 29,0247°(N), 37,0573°(E), 48,0167°(S).

Figure 1: The area of study (Mediterranean) by Google Satellite.

The climate in Mediterranean regions is typified by winter precipitation, with some months exhibiting excess rainfall relative to evapotranspiration. This is followed by warm and dry summer months, during which time there is a deficit in moisture, resulting in the drying out of soils and their annual vegetation. This is known as a xeric moisture regime. They are in the western regions of all continents, situated between the cooler temperature zone and the hot, arid desert zone. The largest Mediterranean region, which surrounds the Mediterranean Sea, covers an area of 2.500.000 km^2 and exhibits a wide variety of soil types and geo-ecosystems. The area's distinctive character is shaped by three key features: its unique climate and vegetation, its rich biodiversity and diverse landscapes and the fragility of the land and its vulnerability to environmental pressures, including drought, hydric erosion, floods, salinization, and the presences of rugged mountains[9].

The mean lowest temperatures for the coldest month are typically between 0 and +3°C, although is some locations, such as desert fringes, the range can extend to +8°C to +9°C, while

[9] Lisetskii F.N. [*et al*.] "Catena linking of landscape-geochemical processes and reconstruction of pedosedimentogenesis," *CATENA*, vol. 28, no. 3-4,2020, p.157-169. DOI: https://doi.org/10.1016/j.catena.2019.104300 [Consulted 08/04/2024]

in the higher mountains, it can reach as low -8°C to -10°C. Additionally, the highest temperatures on hot days can exceed +40°C. The Mediterranean region exhibits considerable variability in rainfall, with mean annual values ranging from 100mm to 2000mm. The lowest recorded values are found at the margins of deserts, particularly in North Africa and the Near East. A precipitation level below 100mm per year represents the borderline between the Mediterranean and desert climates. Rainfall exceeding 1.500mm is predominantly concentrated in coastal mountain ranges. A further distinctive feature of the Mediterranean region is the significant role that agriculture plays in the socioterritorial balance of the states that comprise it. This is particularly evident in the considerable proportion of the regional population that resides in rural areas: at present 36% of the 454 million inhabitants of the region live in such environments. The proportion of the population residing in rural areas is as high as 41% along the southern shore, with the rural population in several countries (notably Egypt, Syria, and Palestinian Territories) continuing to grow at a rate that contrasts with the decline observed in the northern shore. This indicates that in 2020, one- third of the Mediterranean population will continue to reside in the region, with 48 million individuals located on the southern shore. However, the extent of the urban expansion is such that rural populations throughout the region are experiencing a decline in comparison with their urban counterparts. Consequently, the proportion of the population residing in urban areas has increased from half in 1990 to two-thirds at the present time[10].

In recent decades, the Mediterranean region has experienced a faster rate of temperature increase than the global average. Model projections indicate a continued warming and drying trend, with an increased likelihood of heat waves and dry spells. Moreover, countries situated around the Mediterranean basin exhibit considerable disparities, as evidenced by a multitude of socioeconomic and environmental indicators, including per capita gross domestic product (GDP), energy supply CO_2 emissions and water availability. The prevalence of environmental issues is compounded by the social context, given the high population density of the region, with numerous Middle Eastern and North Africa (MENA) countries projected to double their population by the mid-twenty-first century. A growing dependence on irrigation in MENA countries will likely increase their economic and social vulnerability, due to the anticipated reduction in total water availability and the rapid growth of competing urban water demands[11].

2.2 Datasets and Data Processing methodology

A total of thirteen data were collected to calculate indicators. These data arrived at a proper format, so that indicators could be calculated were processed appropriately. The analysis of the data was done in detail in Tables 1-4.

[10] S. Harris, [*et al.*], "Temperate Ecosystems" in (Ed. Burley Jeffery) *Encyclopedia of Forest Sciences*, 2004, Massachusetts, Elsevier, p. 1414-1458, accessible by https://www.sciencedirect.com/referencework/9780121451608/encyclopedia-of-forest-sciences [Consulted 09/04/2024]

[11] Žiga Malek, [*et al.*],"Global change effects on land management in the Mediterranean region", *Global Environmental Change,* Vol. 50, May 2018, p.238-254. DOI: https://doi.org/10.1016/j.gloenvcha.2018.04.007 [Consulted 01/04/2024]

First, a rectangle was created (see Figure 1) to delineate the area of interest and facilitate the subsequent analyses. The coordinates of this polygon are 9,6662°(W), 29,0247°(N), 37,0573°(E), 48,0167°(S). Subsequently, data were collected at five-year intervals between 2000 and 2020 at a spatial resolution of 30 arc-second (~1km at the equator), 0.1°, 0.5 x 0.625°, 0.25, depending on the type of data, by the GPM, MERRA-2 Model and GLDAS Model satellites. To facilitate the performance of operations between the parameters, all pixels in the files were converted to a uniform size (0.008 x 0.008). Once all pixels have been resized according to their values, the maximum and minimum values are retained to create the requisite classes. Specifically, the objective is to create four classes (1,2,3,4) using the following formula: the resulting value is obtained by subtracting the minimum value from the maximum value and dividing the result by four. This value is then added to the minimum value four times, resulting in a new value that is added to the largest value. The resulting file will contain pixels with values 1,2,3 and 4. These values represent the environmental sensitivity of the geographical area represented by the pixel. A value of 1 indicates resilience, whereas a value 4 represents high environmental sensitivity, indicating fragility and risk of degradation and alteration.

Table 1: The following parameters are used to calculate the Climate Quality Index (CQI)

Parameter	Data Range	Class	Score	Description
Precipitation (mm)	15.46-2947.29	14-747.5 747.5-1481 1481-2214.5 2214.5-2948	4 3 2 1	Rainfall rate is a measure of the intensity of rainfall. It is measured by calculating the amount of rain that falls to the earth surface per unit area per unit of time. Data Range: 2000-2020 Spatial analysis: 0.1° Satellite: GPM
Aspect	0-359.97	0-90 90-180 180-270 270-360	1 2 3 4	Aspect is the compass direction that the slope of the terrain faces.

Precipitation is the process where water vapor condenses in the atmosphere to form water droplets that fall to the Earth as rain, sleet, snow, and hail. 'Precipitation' encompasses all the forms of water which falls on the Earth's surface from the atmosphere. Convective Precipitation is precipitation from convective clouds, generally considered to be synonymous with showers[12]. Precipitation was taken from GPM satellite[13].

An *aspect* of 0 means that the slope is North-facing, 90 East-facing, 180 South-facing, and 270 West-facing. Aspect describes how a location is oriented in relation to the cardinal directions (north, south, east, west)[12]. The Copernicus Digital Elevation Model (DEM) for Europe at 100m

[12] NASA, "GIOVANNI", Earth Data, 2024. https://giovanni.gsfc.nasa.gov/giovanni/#service=TmAvMp&starttime=2020-01-01T00:00:00Z&endtime=2023-12-31T23:59:59Z [Consulted 24/02/2024]

[13] Huffman George, " Global Precipitation Measurement Mission", *Global Precipitation Measurement,* NASA, 2014, accessible by https://gpm.nasa.gov/missions/GPM [Consulted 01/04/2024]

resolution (EU-LAEA) derived from Copernicus Global 30m DEM dataset was used to calculate the *aspect* in QGIS.

Table 2: The following parameters are used to calculate the Demographic Index.

Parameter	Data Range	Class	Score	Description
Population Density	0-34275.29	0-8569 8569-17138 17138-25707 25707-34276	1 2 3 4	The Gridded Population of the World, Version 4 (GPWv4): Population Density, Revision 11 consists of estimates of human population density (number of persons per square kilometer) based on counts consistent with national censuses and population registers, for the years 2000, 2005, 2010, 2015, and 2020.
Population Count	0-22225.58	0-5556.5 5556.5-11113 11113-16669.5 16669.5-22226	1 2 3 4	The native 30 arc-second resolution data were aggregated to four lower resolutions (2.5 arcminute, 15 arc-minute, 30 arc-minute, and 1 degree) Data Range: 2000-2020.

The result is based on census data[14].

Table 3: The following parameters are used to calculate the Soil Quality Index.

Parameter	Data Range	Class	Score	Description
Soil Moisture Content ($kg \cdot m^{-2}$)	3.06-44.38	2-12.75 12.75-23.5 23.5-34.25 34.25-45	4 3 2 1	Average layer soil moisture is the depth-averaged amount of water present in a specific soil layer beneath the surface. Data Range: 2000-2020 Spatial: 0.25 ° x 0.25 ° Underground: 0-10km Satellite: GLDAS
Slope (°)	0-89.99	0-22.5 22.5-45 45-67.5 67.5-90	1 2 3 4	Slope informs about how steep the terrain is.
Average Surface Skin Temperature (K)	268.20-300.66	267-275.5 275.5-284 284-292.5 292.5-301	1 2 3 4	The average temperature of the Earth's surface. Spatial: 0.25 ° x 0.25 ° Data Range: 2000-2020 Satellite: GLDAS
Soil Temperature (K)	271.36-300.62	270-277.75 277.75-285.5 285.5-293.25 293.25-301	1 2 3 4	Average layer soil temperature is the depth-averaged temperature beneath the soil surface at a specified layer. Spatial: 0.25 ° x 0.25 ° Data Range: 2000-2020 Satellite: GLDAS

[14] NASA, "Socioeconomic Data and Applications Center", 30/08/2015. accessible by https://sedac.ciesin.columbia.edu/data/collection/gpw-v4/sets/browse. [Consulted 04/02/2024]

Soil moisture content can be measured as Gravimetric Soil Moisture (GSM). GSM is the mass of water compared to the mass of solid materials per unit volume of soil. Soil moisture can also be expressed as Volumetric Soil Moisture (VSM) which is the volume of water per unit volume of soil. As water is of a known density, the mass of water per unit volume of soil (g/cm^3) can be easily determined. Water storage refers to the amount of water retained in a hydrologic division (such as a watershed, soil layer, or geographic region), in contrast to moving water, which is surface or subsurface runoff or groundwater.

The Copernicus Digital Elevation Model (DEM) for Europe at 100m resolution (EU-LAEA) derived from Copernicus Global 30m DEM dataset was used to calculate the *slope* in QGIS.

Average surface skin temperature is the actual temperature of the surface, and it can be considerably different than the air temperature above the surface, particularly in warm, sunny conditions.

Soil temperatures may contribute to the low frequency variability of energy and water fluxes. They are important measured quantities in analyzing of the ground heat flux, and then the energy and water cycles[15].

Table 4: The following parameters are used to calculate the Vegetation Quality Index.

Parameter	Data Range	Class	Score	Description
Land Cover	10-220	9-62 62-115 115-168 168-221	1 2 3 4	Each pixel value corresponds to the label of a land cover class defined using UN-LCCS classifiers. Data Range: 2000-2020 Spatial: 300m
Greenness Fraction	0-0.95	0-0.25 0.25-0.5 0.5-0.75 0.75-1	4 3 2 1	Vegetation refers to the ground cover provided by plants. Spatial: 0.5 ° x 0.625 ° Data Range: 2000-2020 Satellite: MERRA-2

[15] NASA, "GIOVANNI", Earth Data, 2024. https://giovanni.gsfc.nasa.gov/giovanni/#service=TmAvMp&starttime=2020-01-01T00:00:00Z&endtime=2023-12-31T23:59:59Z [Consulted 24/02/2024]

VALUE	LABEL	COLOR
0	No Data	
10	Cropland, rainfed	
20	Cropland, irrigated or post-flooding	
30	Mosaic cropland (>50%) / natural vegetation (tree, shrub, herbaceous cover) (<50%)	
40	Mosaic natural vegetation (tree, shrub, herbaceous cover) (>50%) / cropland (<50%)	
50	Tree cover, broadleaved, evergreen, closed to open (>15%)	
60	Tree cover, broadleaved, deciduous, closed to open (>15%)	
70	Tree cover, needleleaved, evergreen, closed to open (>15%)	
80	Tree cover, needleleaved, deciduous, closed to open (>15%)	
90	Tree cover, mixed leaf type (broadleaved and needleleaved)	
100	Mosaic tree and shrub (>50%) / herbaceous cover (<50%)	
110	Mosaic herbaceous cover (>50%) / tree and shrub (<50%)	
120	Shrubland	
130	Grassland	
140	Lichens and mosses	
150	Sparse vegetation (tree, shrub, herbaceous cover) (<15%)	
160	Tree cover, flooded, fresh or brakish water	
170	Tree cover, flooded, saline water	
180	Shrub or herbaceous cover, flooded, fresh/saline/brakish water	
190	Urban areas	
200	Bare areas	
210	Water bodies	
220	Permanent snow and ice	

Figure 2: Land Cover data[16] [14]

Land cover comes from the combination of Envisat's MERIS satellite[17] from 2000 to 2012 and then from the Sentinel-2 of the Copernicus program[18].

Vegetation cover is measured in Enhanced Vegetation Index (EVI), Normalized Difference Vegetation Index (NDVI), or fractional coverage. The mathematical formula for NDVI is:

$\text{NDVI} = \frac{(\text{NIR} - \text{VIS})}{(\text{NIR} + \text{VIS})}$, where NIR is near-infrared radiation and VIS is visible wavelength radiation. EVI uses a similar formula to that of NDVI, but also performs an atmospheric correction.

The greenness fraction was taken from MERRA-2 satellite[19].

[16] Kandice L. [*et al.*], "A 29-year time series of annual 300 m resolution plant-functional-type maps for climate models", *Earth Syst. Sci. Data,* vol. 15, May 2023, p.1465 – 1499.
[17] European Space Agency, " Explore MERIS - Earth Online", *MERIS Applications*, 2022, accessible by https://earth.esa.int/eogateway/instruments/meris [Consulted 09/06/2024]
[18] European Space Agency, " Sentinel-2", *S2 Mission,* accessible by https://sentiwiki.copernicus.eu/web/s2-mission [Consulted 09/05/2024]
[19] Pawson Steven, " MERRA-2 ", *Modern-Era Retrospective analysis for Research and Applications, Version 2*, NASA, September 2022, accessible by https://gmao.gsfc.nasa.gov/reanalysis/MERRA-2/ [Consulted 12/06/2024]

Table 5: The following parameters are used to calculate the Energy Exchange Index.

Parameter	Data Range	Class	Score	Description
Albedo (%)	8.66-59.80	7-20.25 20.25-33.5 33.5-46.75 46.75-60	1 2 3 4	Albedo is the ratio of the incident solar radiation that is reflected by a surface to that incident on it. Spatial: 0.25 ° x 0.25 ° Data Range: 2000-2020 Satellite: GLDAS
Latent Heat Net Flux ($W \cdot m^{-2}$)	1.12-83.84	0-21 21-42 42-63 63-84	1 2 3 4	Heat flux is the rate at which heat, or thermal energy, is transferred through a given surface. Spatial: 0.25 ° x 0.25 ° Data Range: 2000-2020 Satellite: GLDAS
Evapotranspiration ($kg \cdot m^{-2} \cdot s^{-2}$)	$1 \cdot 10^{-6}$- $34 \cdot 10^{-6}$	0-$8.75 \cdot 10^{-6}$ $8.75 \cdot 10^{-6}$- $1.75 \cdot 10^{-6}$ $1.75 \cdot 10^{-5}$- $2.625 \cdot 10^{-5}$ $2.625 \cdot 10^{-5}$- $3.5 \cdot 10^{-5}$	4 3 2 1	Total Evapotranspiration (ET) is the sum of evaporation and plant transpiration. Spatial: 0.25 ° x 0.25 ° Data Range: 2000-2020 Satellite: GLDAS

Clouds are the chief cause of variations in the Earths *albedo* since clouds have highly varying albedo, dependent upon thickness and composition. The albedo of old snow is about 55% (0.55) and new snow around 80% (0.8). Water surfaces vary from very low, about 5% (0.05) at high sun elevation, to at least 70% (0.70) at low sun angles. In radiative transfer studies, single scattering albedo is the ratio of scattering optical depth to the total optical depth (scattering + extinction) of the atmosphere. It is a dimensionless quantity and ranges from 0 to 1. Reflectance is the ratio of incident radiation that is reflected by a surface as a function of the wavelength of the radiation.

In Earth systems, there are three major types of heat flux: ground heat flux, *latent heat flux*, and sensible heat flux. Ground heat flux is the process where heat energy is transferred from the Earth's surface to the subsurface of the Earth via conduction. It is a vital component of the Earth's surface energy budget. Ground heat flux can be presented by the amount of heat transmitted per unit of area per unit of time. Latent heat flux is the flux of heat from the Earth's surface to the atmosphere that is associated with evaporation of water at the surface and subsequent condensation of water vapor in the troposphere. Latent heat flux is commonly measured with the Bowen ratio technique, or by eddy covariance. Sensible heat flux is the process where heat energy is transferred from the Earth's surface to the atmosphere by conduction and convection. The heat energy then can move horizontally by atmospheric circulation. Sensible heat flux can be expressed by the amount of heat transmitted per unit of area per unit of time.

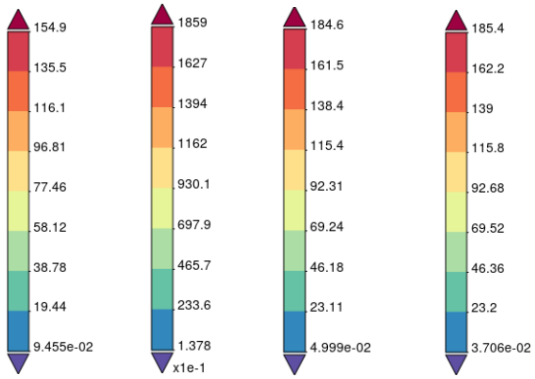

Figure 3: Max-min range of Latent Heat Net Flux data

Evaporation accounts for the movement of water to the air from various sources on Earth's surface, such as soil, ocean, etc. Transpiration accounts for the movement of water within a plant and the subsequent loss of water as vapor departs through leaves. The evapotranspiration rate expresses the amount of water lost from a unit area of surface per unit time. The time unit can be an hour, day, month, year, or even a decade.

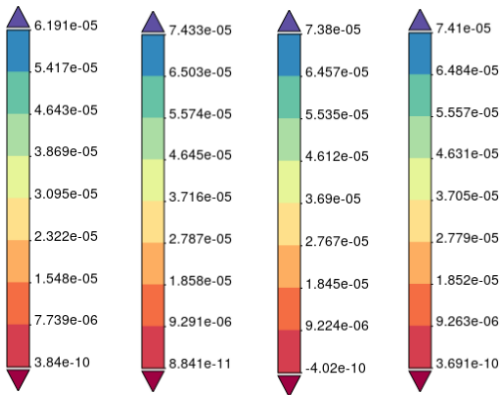

Figure 4: Max-min range of Evapotranspiration data

2.3 Environmental Sensitivity

The environmental sensitivity of the Mediterranean region represents a significant challenge that requires urgent attention. To assess and manage the sensitivity, two key tools were calculated: the Environmental Sensitivity Areas Index (ESAI) and the Quality Index (QI). The ESAI provides a comprehensive framework for the identification of areas most sustainable to degradation, considering a range of factors, including soil quality, climate, vegetation, and human impact. In essence, several different environmental indicators are aggregated into a single final indicator, which represents the areas that are most susceptible to land degradation. Furthermore, the QI assesses the overall environmental health of these areas, thereby providing information on their resilience or vulnerability to further degradation. The objective of this chapter is to analyze the indicators to ascertain the spatial distribution of environmental

sensitivity in the Mediterranean and to propose conservation and sustainable land management practices.

The indices were calculated using equations (1) and (2):

$$(1)\quad \mathrm{QI_{ij}} = (\mathrm{V_{1ij}} \times \mathrm{V_{2ij}} \times \ldots \times \mathrm{V_{nij}})^{\frac{1}{n}}$$

Where $\mathrm{QI_{ij}}$ represents pixel values of the QI, $\mathrm{V_{nij}}$ is the score value of a pixel in the position ("i,j") regarding the reclassified parameter and "n" is the number of the used parameters define each QI (Tables 1-5).

$$(2)\quad \mathrm{ESAI_{ij}} = \mathrm{QI_{1ij}} \times \mathrm{QI_{2ij}} \times \ldots \times \mathrm{QI_{nij}})^{\frac{1}{n}}$$

Where $\mathrm{ESAI_{ij}}$ is the pixel value of the final index, whereas QI_{nij} represents pixel values of each of the defined QIs and "n" is the number of the QIs were used to calculate the ESAI.

Five different categories of indicators have been selected based on equations (1) and (2). These indicators are called Climate Quality Index (CQI), Demographic Index (DI), Soil Quality Index (SQI), Vegetation Quality Index (VQI) and Exchange Index (EI). Specifically, the CQI was evaluated using two parameters, Precipitation and Aspect. These parameters are listed in Table 1, which provides the calibration values associated with the different value ranges for each parameter and a description of the data sets. For the DE index, the parameters Population Density and Population Count were used (Table 2). The parameters used for the SQI were Soil Moisture Content, Slope, Average Surface Skin Temperature and Soil Temperature, as detailed in Table 3. The VQI was calculated based on Land Cover and Greenness Fraction, as shown in Table 4. Finally, EI was calculated from the parameters Albedo, Latent Heat Net Flux and Evapotranspiration, with the relative values given in Table 5.

3. RESULTS

The results present the findings of a survey on the status of degraded areas in the Mediterranean, employing the ESAI index. The analysis is centered on the outcomes of each indicator utilized in the calculation of the ESAI (Figure 30-34). The data collection and processing stages allow for the identification of the primary causes and consequences of degradation, as well as the potential avenues for sustainable development of these areas.

3.1 Climate quality index

The Climate Quality Index (CQI) was devised based on precipitation and aspect (Table 1), thus providing an overall assessment of climate conditions. As illustrated in Figures 2-6, the climate values are represented by color according to Table 1, with red indicating areas of high resilience and blue representing high environmental sensitivity. It can be observed that the northern Mediterranean countries exhibit superior climatic conditions in comparison to those in Africa, due to a combination of geographical, meteorological, and environmental factors. It is evident that Spain, France Italy, and Balkan countries situated in the Mediterranean experience rainfall and sunshine, whereas the southern Mediterranean, including Egypt, Libya, Tunisia, Algeria and Marocco, is characterized by a dry and arid climate, desolation, minimal rainfall, high temperatures and low humidity. The climate in the northern Mediterranean is therefore milder, which has resulted in the regions becoming fertile. In contrast, the climate in the southern Mediterranean is drier, which has had a negative impact on the quality of life.

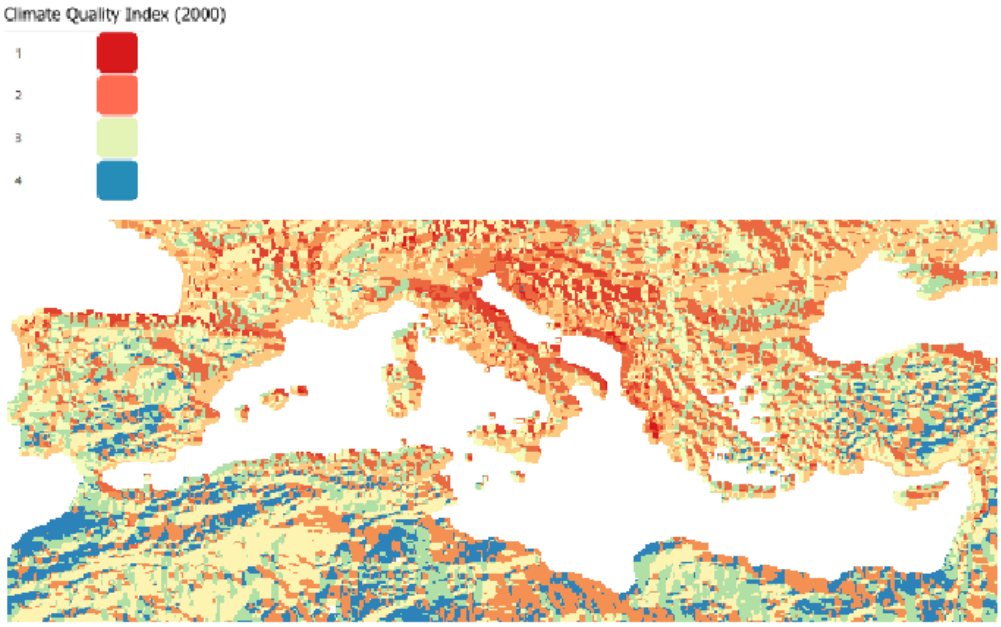

Figure 5: Climate Quality Index (CQI) spatial distribution in 2000. The four different colored ranges of values represent four sensitivity stages - "very low", "low", "high" and "very high" from the minimum to the maximum range of values.

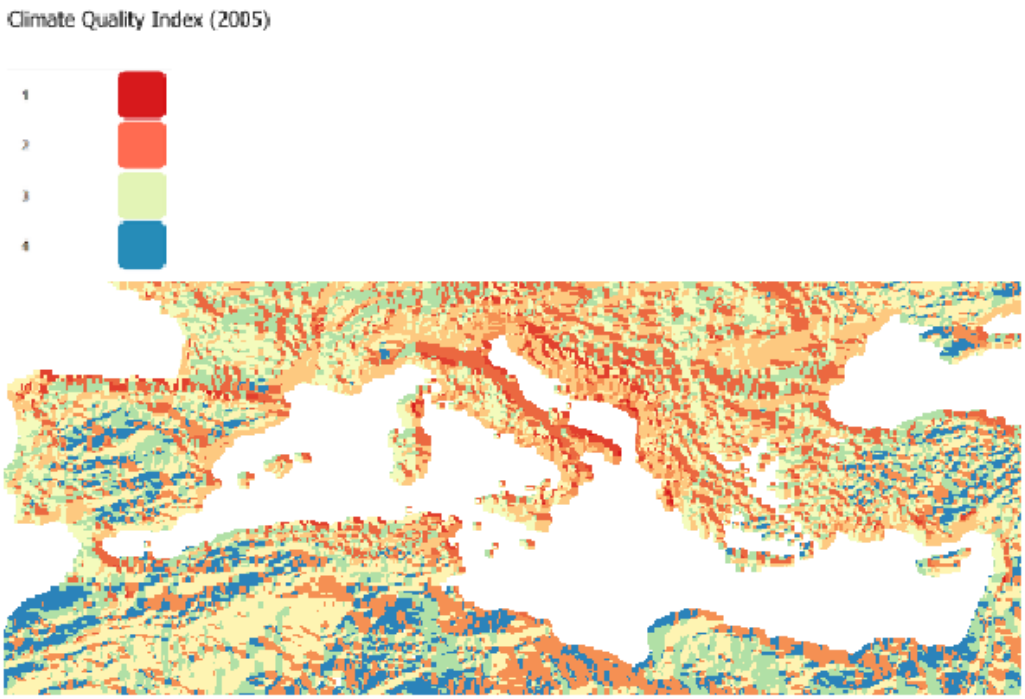

Figure 6: Climate Quality Index (CQI) spatial distribution in 2005. The four different colored ranges of values represent four sensitivity stages - "very low", "low", "high" and "very high" from the minimum to the maximum range of values.

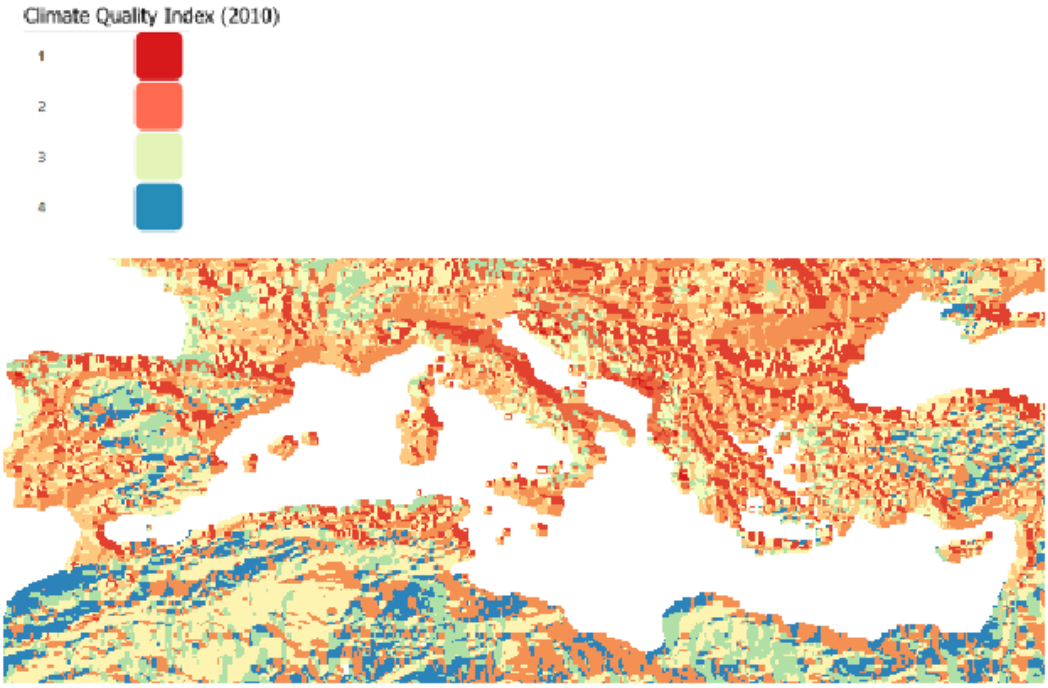

Figure 7: Climate Quality Index (CQI) spatial distribution in 2010. The four different colored ranges of values represent four sensitivity stages - "very low", "low", "high" and "very high" from the minimum to the maximum range of values.

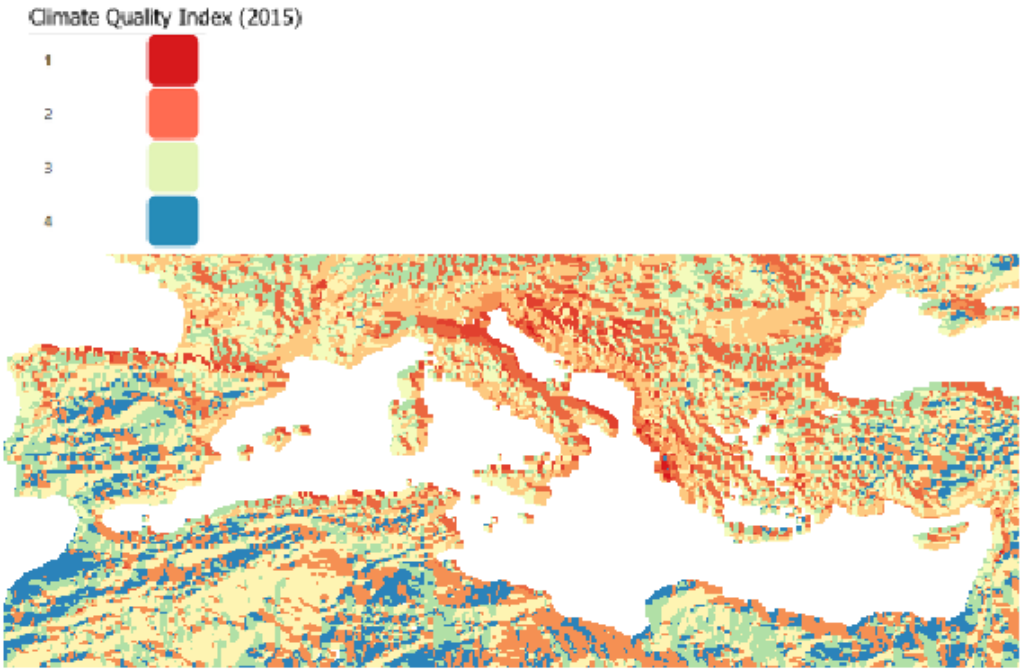

Figure 8: Climate Quality Index (CQI) spatial distribution in 2015. The four different colored ranges of values represent four sensitivity stages - "very low", "low", "high" and "very high" from the minimum to the maximum range of values.

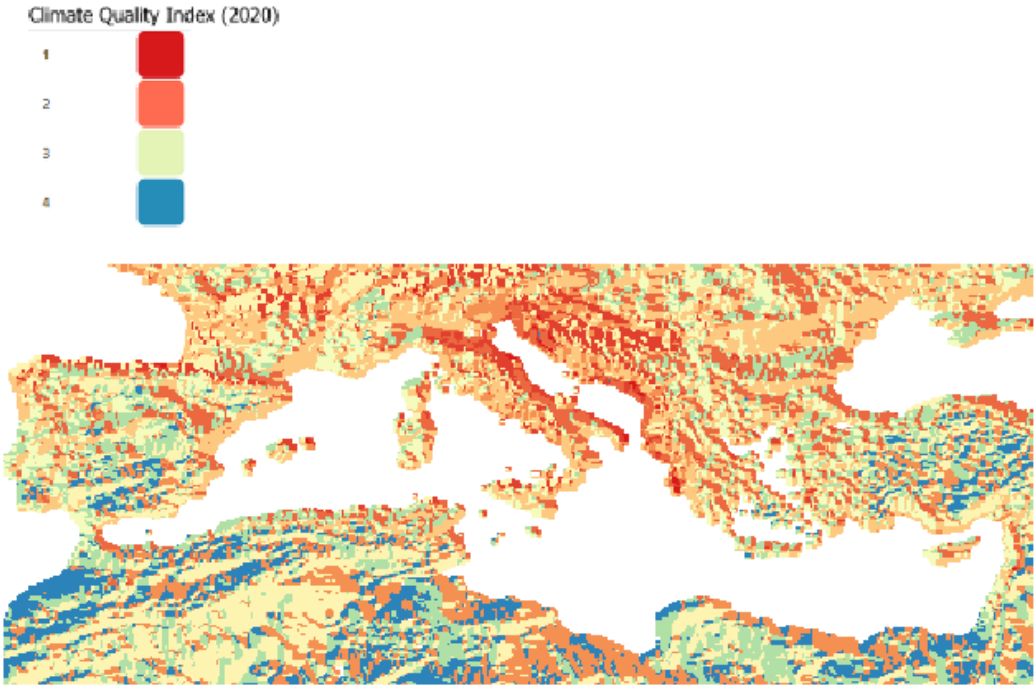

Figure 9: Climate Quality Index (CQI) spatial distribution in 2020. The four different colored ranges of values represent four sensitivity stages - "very low", "low", "high" and "very high" from the minimum to the maximum range of values.

A comparison of Figures 2-6 reveals that there have been noticeable changes in the Mediterranean climate between 2000 and 2020, with increased climate sensitivity, particularly in the northern countries, where rainfall has decreased, with many areas experiencing drought.

3.2 Demographic index

The Demography Index (DI) is comprised of two components: Population Density and Population Count[20] in Table 2. Figures 7-11 illustrate the spatial distribution of the index values for the years 2000, 2005, 2010 and 2020. In practical, the various colors employed on the map are indicative of specific values pertaining to the density and distribution of the population. Specifically, pixels indicated in red correspond to a normal population distribution, whereas those indicated in blue correspond to areas of overpopulation. The values associated with these areas are detailed in Table 2. The analysis of the maps reveals a gradual increase in population in urban areas between 2000 and 2020. This is evidenced by the predominance of the blue color, which is particularly evident in the northeastern Mediterranean countries and Algeria in North Africa. In contrast, the southern part of the Mediterranean, which includes countries such as Egypt, Libya, Tunisia, and Morocco, exhibits lower values in the DI and is therefore represented by a red color, indicating a lack of significant change over time. These regions, while experiencing population growth, have not undergone the same degree of urbanization as northern countries, resulting in a lower population density. The most significant factors contributing to the observed increase in index values are population growth and urbanization. Finally, the period between 2000 and 2020 saw a significant increase in the index, with urbanization and population growth contributing to the reshaping of the demographic landscape of the Mediterranean. The maps in Figures 7-11 illustrate these changes and highlight the regions that have undergone the most significant demographic shifts.

[20] NASA, "Socioeconomic Data and Applications Center", 30/08/2015. accessible by https://sedac.ciesin.columbia.edu/data/collection/gpw-v4/sets/browse. [Consulted 04/02/2024]

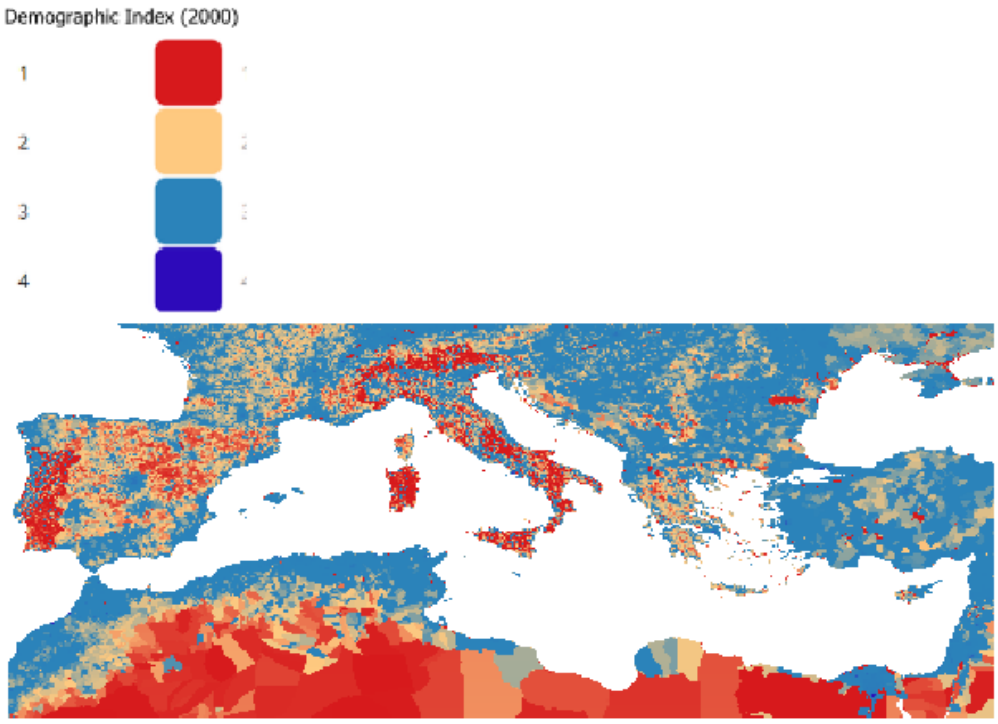

Figure 10: Demographic Index (DI) spatial distribution in 2000. The four different colored ranges of values represent four sensitivity stages - "very low", "low", "high" and "very high" from the minimum to the maximum range of values.

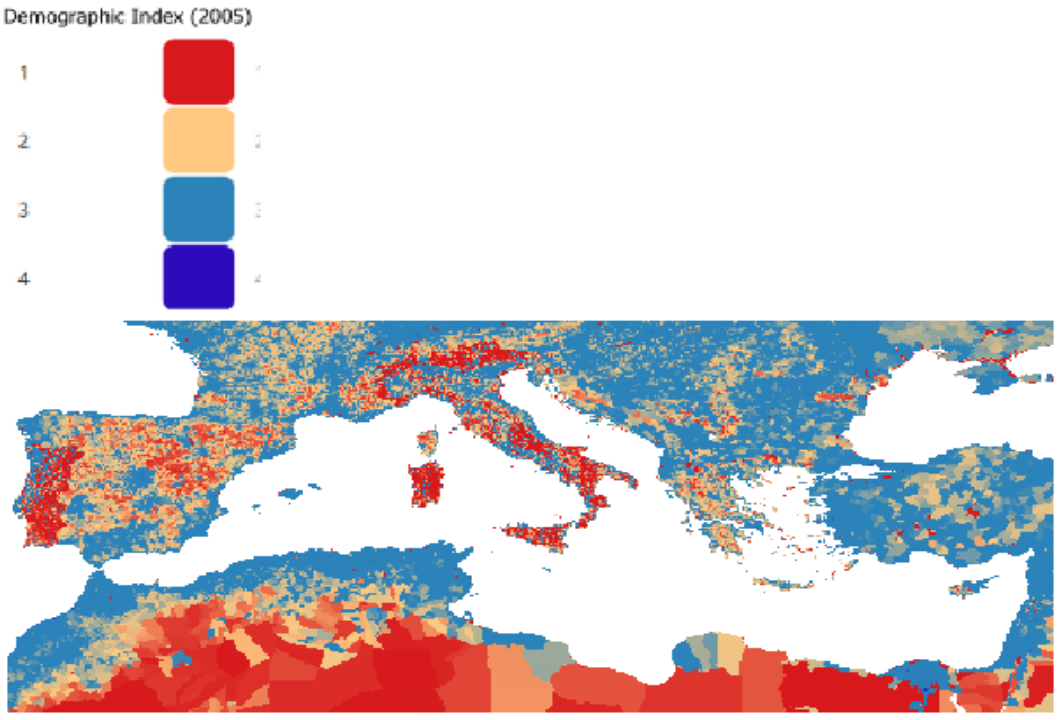

Figure 11: Demographic Index (DI) spatial distribution in 2005. The four different colored ranges of values represent four sensitivity stages - "very low", "low", "high" and "very high" from the minimum to the maximum range of values.

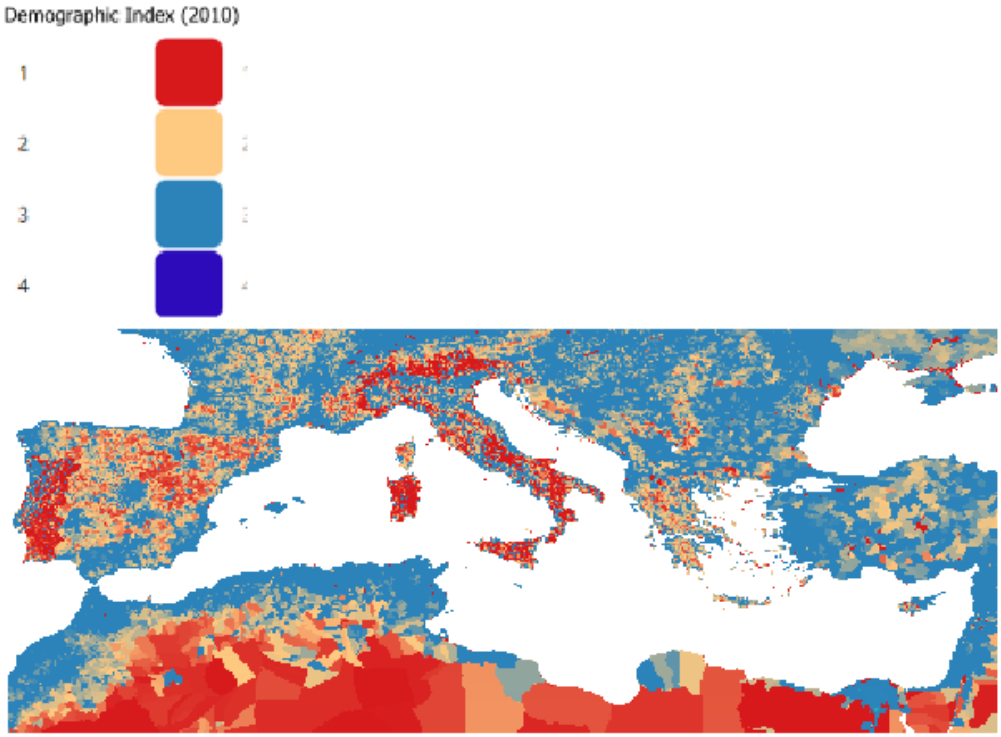

Figure 12: Demographic Index (DI) spatial distribution in 2010. The four different colored ranges of values represent four sensitivity stages - "very low", "low", "high" and "very high" from the minimum to the maximum range of values.

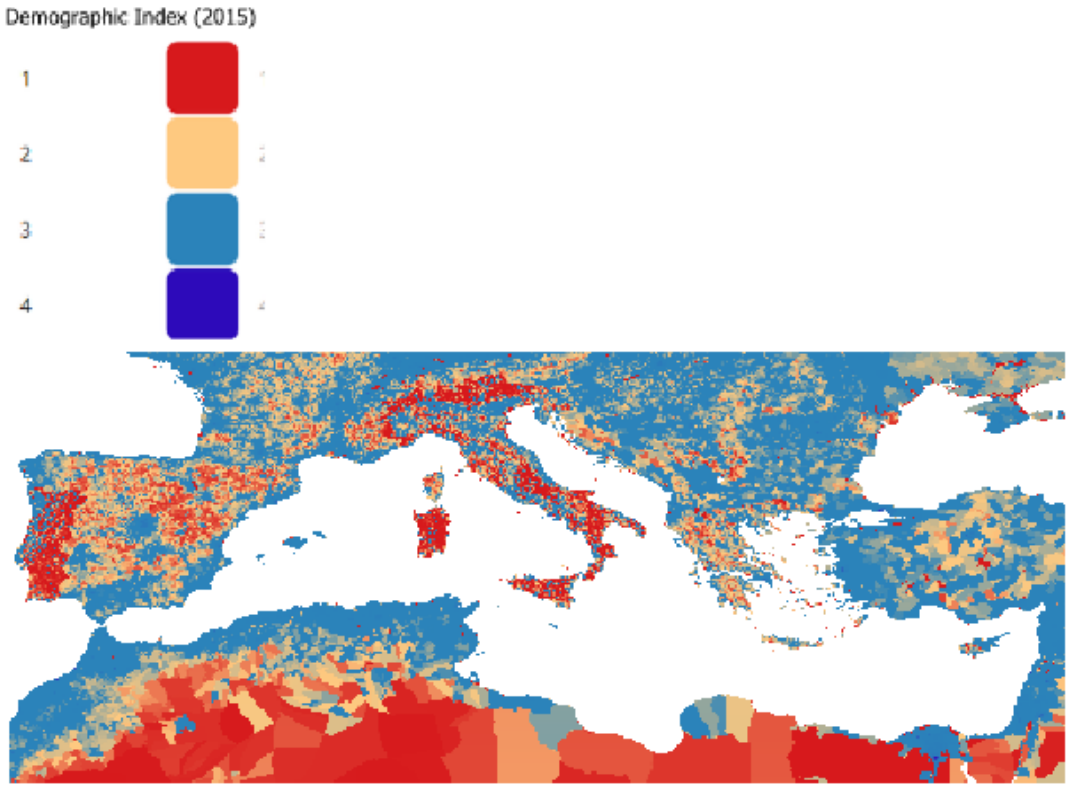

Figure 13: Demographic Index (DI) spatial distribution in 2015. The four different colored ranges of values represent four sensitivity stages - "very low", "low", "high" and "very high" from the minimum to the maximum range of values.

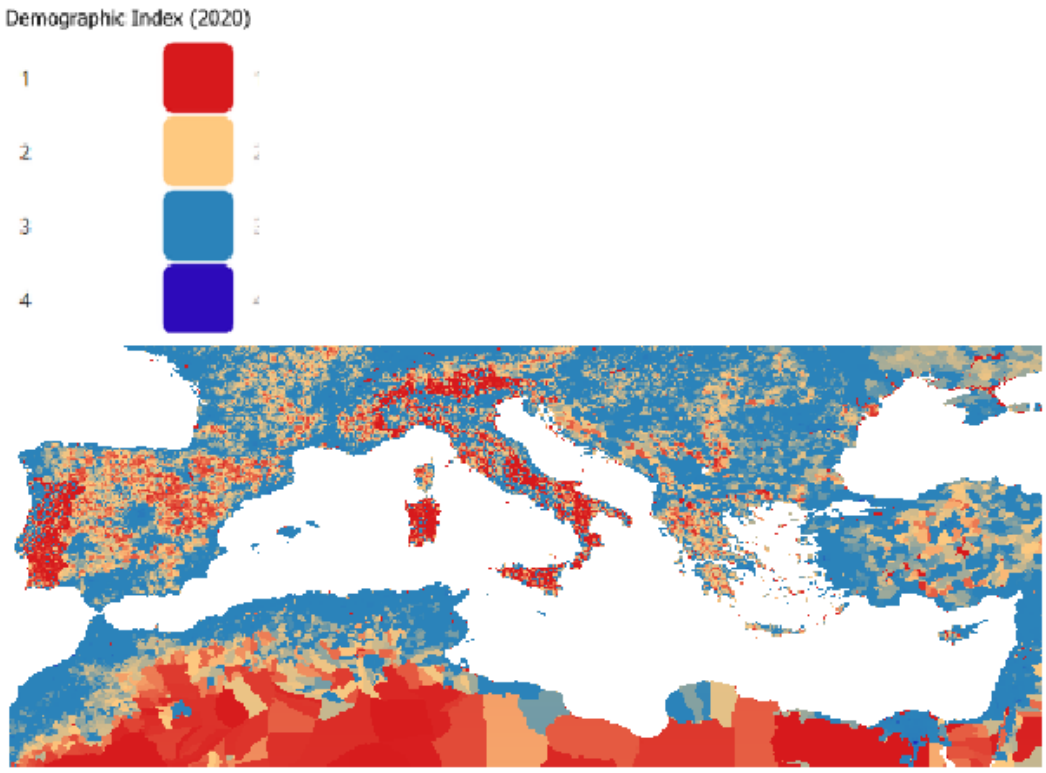

Figure 14: Demographic Index (DI) spatial distribution in 2020. The four different colored ranges of values represent four sensitivity stages - "very low", "low", "high" and "very high" from the minimum to the maximum range of values.

3.3 Soil quality index

The Soil Quality Index (SQI) is comprised of four parameters: Soil Moisture Content, Slope, Average Surface Skin Temperature and Soil Temperature (Table 3). A change in soil moisture content has the potential to impact soil fertility and soil erosion resistance. The impact of slope on erosion, water runoff and vegetation distribution make it a significant factor. Areas with greater slopes are more susceptible to erosion, particularly in regions with minimal vegetative cover and high precipitation levels. A review of the data reveals a notable decline in soil quality across Mediterranean countries over a five-year cycle. The SQI demonstrates considerable fluctuations over the southern countries of the Mediterranean region. These changes reflect the effects of climate change and increasing human activity. An increase in temperature and a reduction in humidity render the soil more vulnerable, particularly in areas with steep slopes. This is because of drought and moisture loss, as well as an increase in the temperature of the soil surface. The combination of soil slope and a reduction in moisture, coupled with an increase in temperature, intensifies soil erosion, especially in the mountainous areas of southern Europe and North Africa (Figure 12-16).

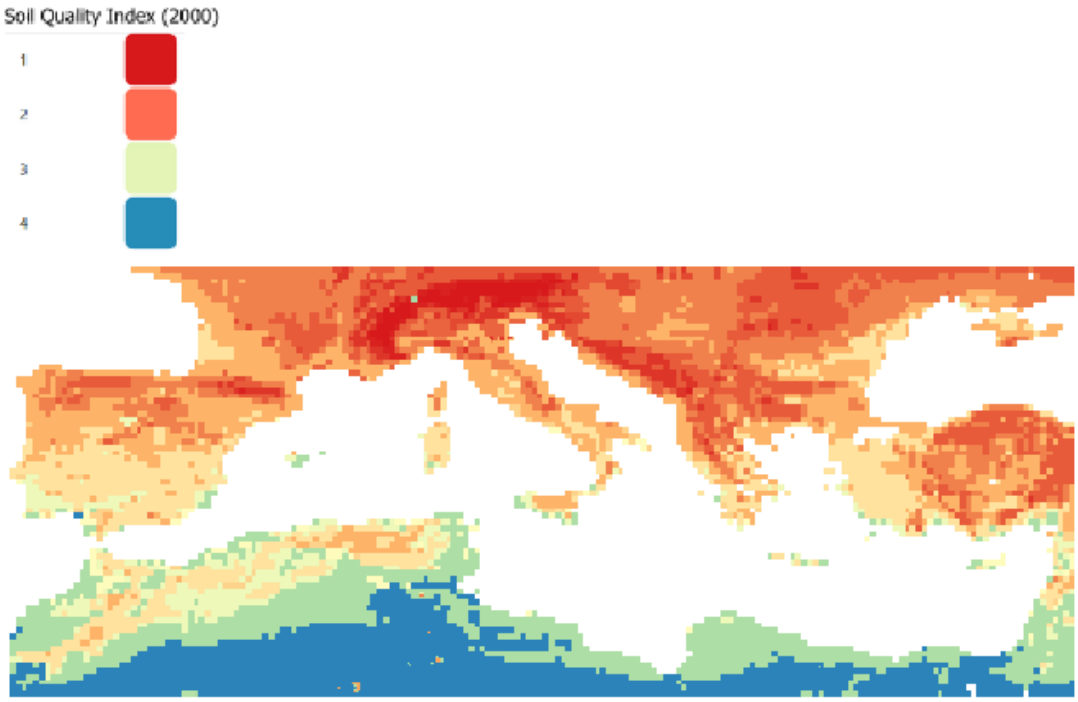

Figure 15: Soil Quality Index (SQI) spatial distribution in 2000. The four different colored ranges of values represent four sensitivity stages - "very low", "low", "high" and "very high" from the minimum to the maximum range of values.

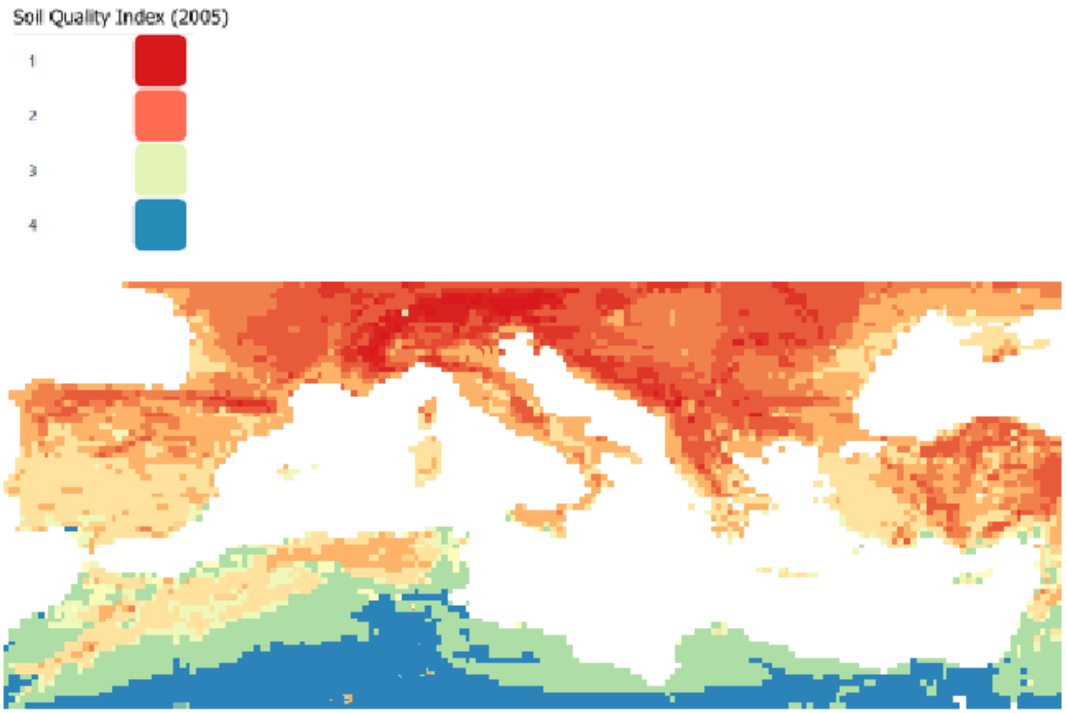

Figure 16: Soil Quality Index (SQI) spatial distribution in 2005. The four different colored ranges of values represent four sensitivity stages - "very low", "low", "high" and "very high" from the minimum to the maximum range of values.

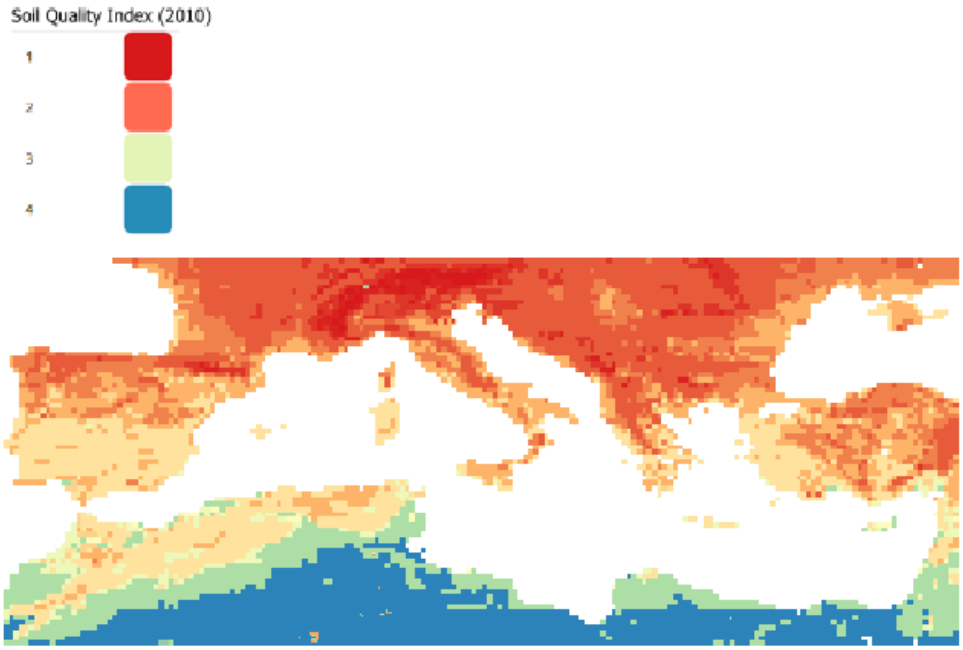

Figure 17: Soil Quality Index (SQI) spatial distribution in 2010. The four different colored ranges of values represent four sensitivity stages - "very low", "low", "high" and "very high" from the minimum to the maximum range of values.

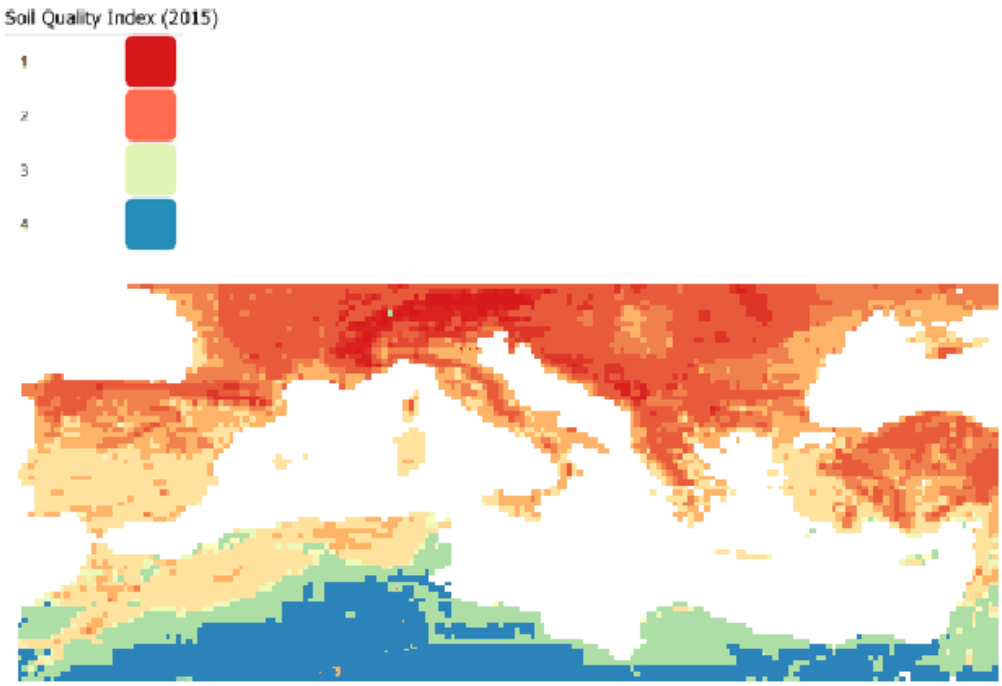

Figure 18: Soil Quality Index (SQI) spatial distribution in 2015. The four different colored ranges of values represent four sensitivity stages - "very low", "low", "high" and "very high" from the minimum to the maximum range of values.

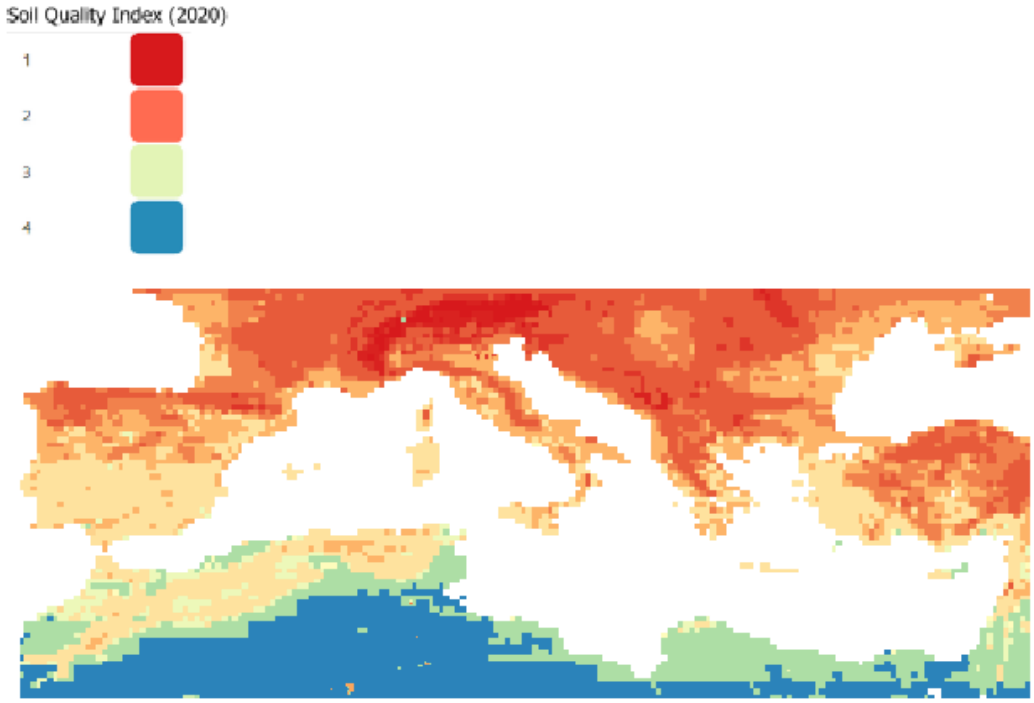

Figure 19: Soil Quality Index (SQI) spatial distribution in 2020. The four different colored ranges of values represent four sensitivity stages - "very low", "low", "high" and "very high" from the minimum to the maximum range of values.

3.4 Vegetation quality index

The Vegetation Quality Index (VQI) is comprised of two components: the Greenness Fraction and Land Cover[21] in Table 4. It is a tool for assessing the resilience and health of soil in different areas. As illustrated in the data presented, the vegetation quality in an area is represented by pixels blue and green (values 4 and 3 respectively), which indicate high quality and resilience. In contrast, pixels displaying red (value 1) indicate areas with high sensitivity, where vegetation quality is low, and degradation is present. Such areas are more susceptible to the impact of natural disasters and changes in land use. A comparison of the data from 2000 to 2020 (Figures 17-21) reveals significant changes in the geographical distribution and quality of vegetation in the Mediterranean. The discrepancy in values between 2000, 2005, 2010, 2015 and 2020 is pronounced, with red prevailing throughout the northern Mediterranean and blue confined to only a portion of Algeria, Libya, and Cyprus, in contrast to 2000 when blue areas were more expansive. This highlights that the overall situation has deteriorated. This discrepancy can be attributed to alterations in land use. The conversion of natural areas to agricultural or urban zones results in the loss of vegetation and heightened erosion. Additionally, tourism in the Mediterranean has precipitated the construction of infrastructure, predominantly in coastal regions. Furthermore, urbanization and fires have contributed to this change. The

[21] ESA, " ESA/CCI viewer ", 2017, accessible by https://maps.elie.ucl.ac.be/CCI/viewer/download.php [Consulted 03/06/2024]

consequences of these factors have resulted in the gradual erosion of soil and resilience reduction to natural disasters.

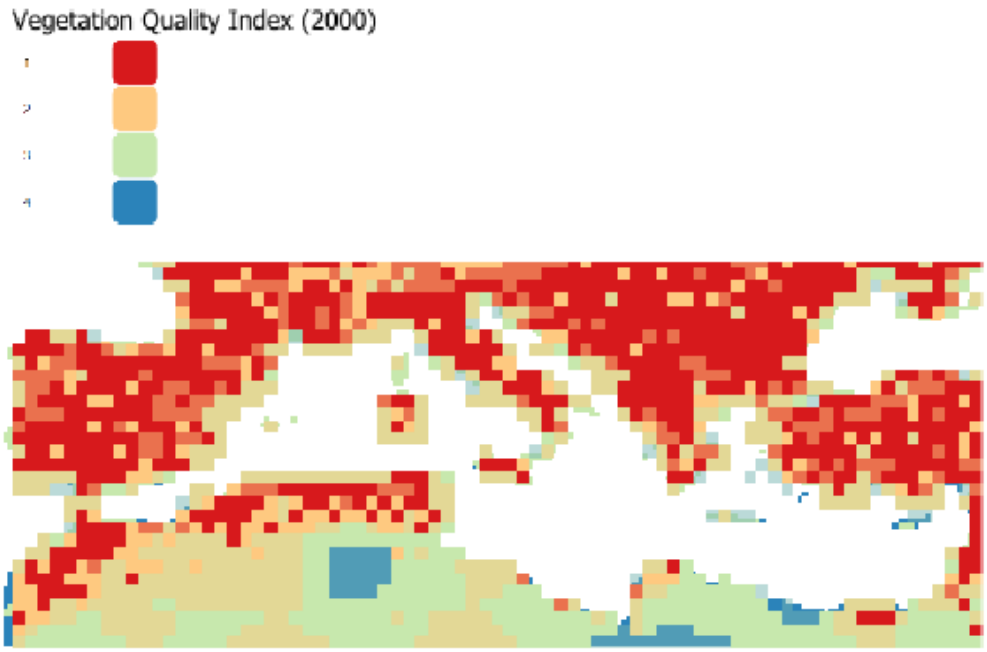

Figure 20: Vegetation Quality Index (VQI) spatial distribution in 2000. The four different colored ranges of values represent four sensitivity stages - "very low", "low", "high" and "very high" from the minimum to the maximum range of values.

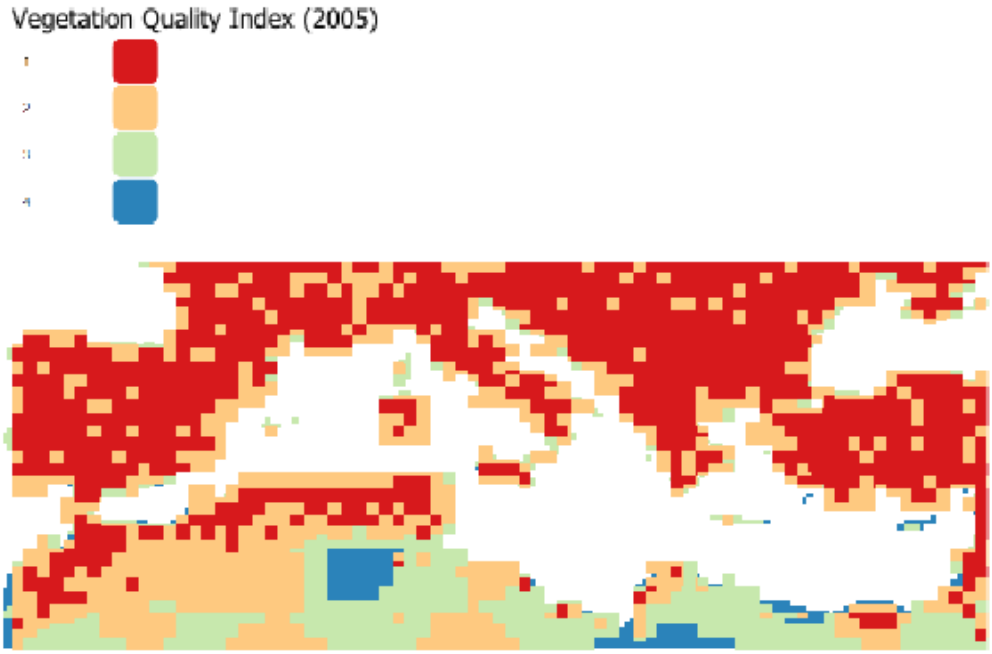

Figure 21: Vegetation Quality Index (VQI) spatial distribution in 2005. The four different colored ranges of values represent four sensitivity stages - "very low", "low", "high" and "very high" from the minimum to the maximum range of values.

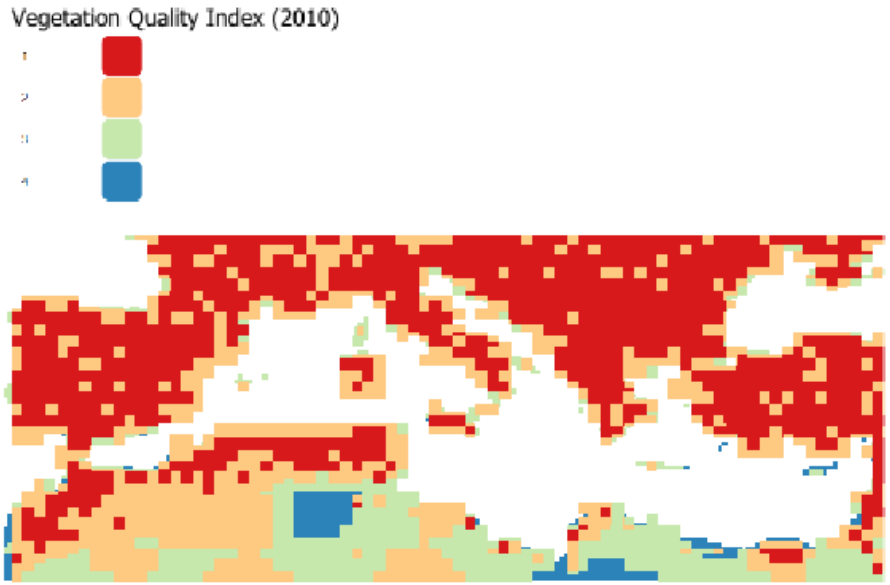

Figure 22: Vegetation Quality Index (VQI) spatial distribution in 2010. The four different colored ranges of values represent four sensitivity stages - "very low", "low", "high" and "very high" from the minimum to the maximum range of values.

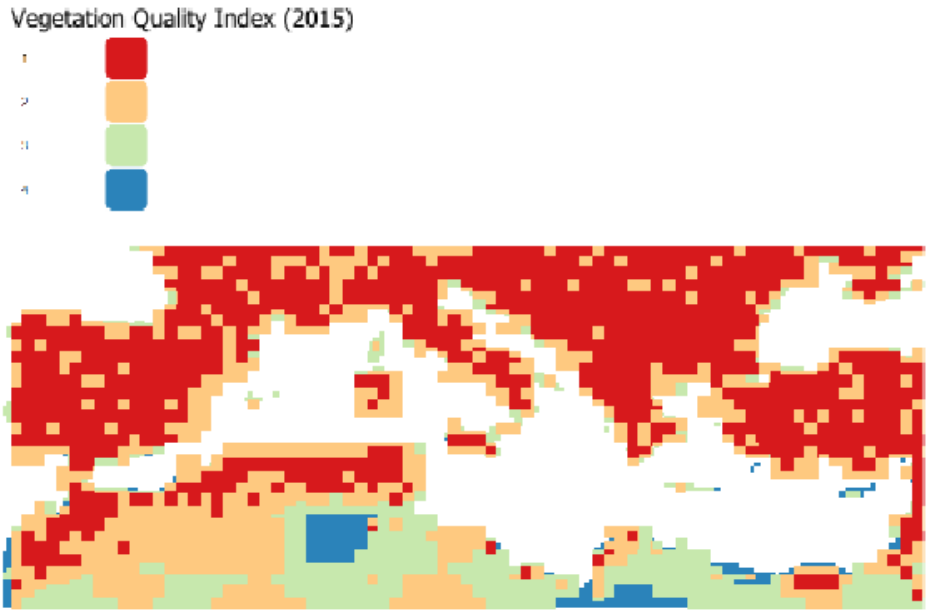

Figure 23: Vegetation Quality Index (VQI) spatial distribution in 2015. The four different colored ranges of values represent four sensitivity stages - "very low", "low", "high" and "very high" from the minimum to the maximum range of values.

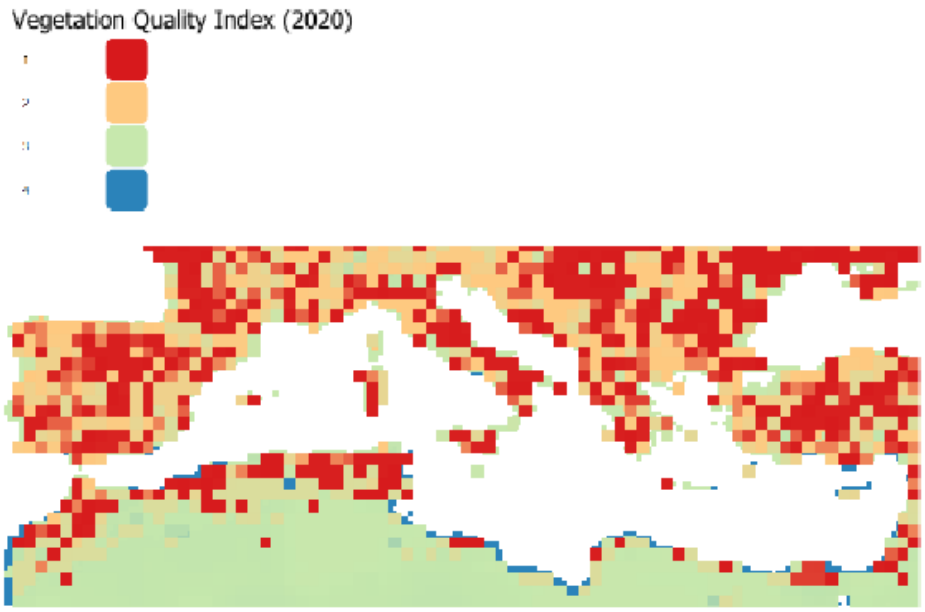

Figure 24: Vegetation Quality Index (VQI) spatial distribution in 2020. The four different colored ranges of values represent four sensitivity stages - "very low", "low", "high" and "very high" from the minimum to the maximum range of values.

3.5 Energy Exchange Index

The Energy Exchange Index (EEI) includes Albedo, Latent Heat Net Flux and Evapotranspiration (Table 5). It can be used to understand the energy fluxes between the Earth's surface and the atmosphere. A surface with a high Albedo reflects a large production of solar radiation, whereas a surface with a low Albedo absorbs most of the radiation and reflects little. Latent Heat Net Flux refers to the amount of energy absorbed or released when a substance changes state and relates to the evaporation of water from the oceans and the Earth's surface, so areas with high Latent Heat Net Flux contribute to increased humidity. Evapotranspiration is the combination of two processes, the evapotranspiration of water from the land surface and transpiration (removal of water vapor) by plants. Evapotranspiration is a function of temperature, humidity, wind, and vegetation. An area with high evaporation is more sensitive to environmental changes, as water loss through this process can affect agricultural production and climate stability. By analyzing these factors (Figure 22-26), it is projected how energy is exchanged between the Earth's surface and the atmosphere. Comparing the years 2000, 2005, 2010, 2015 and 2020, there are small changes in the EEI between 2000 and 2020, but in 2005, 2010 and 2015 the green color (value 3) represents values with high EEI spread over Algeria, Libya, Egypt, northern Italy, part of Turkey and Montenegro.

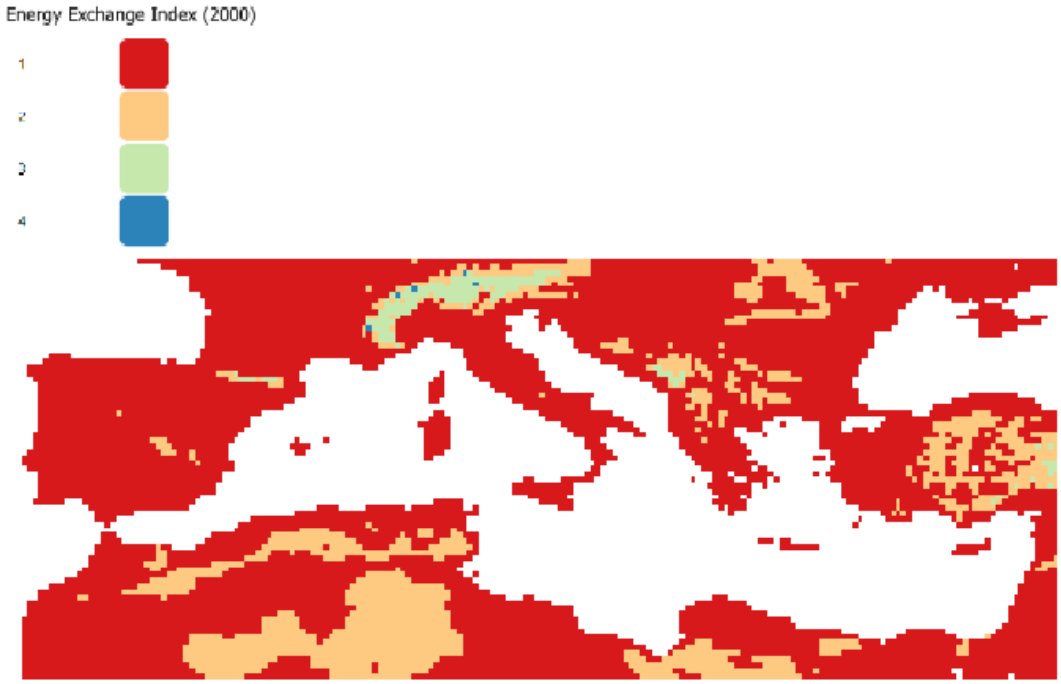

Figure 25: Energy Exchange Index (EEI) spatial distribution in 2000. The four different colored ranges of values represent four sensitivity stages - "very low", "low", "high" and "very high" from the minimum to the maximum range of values.

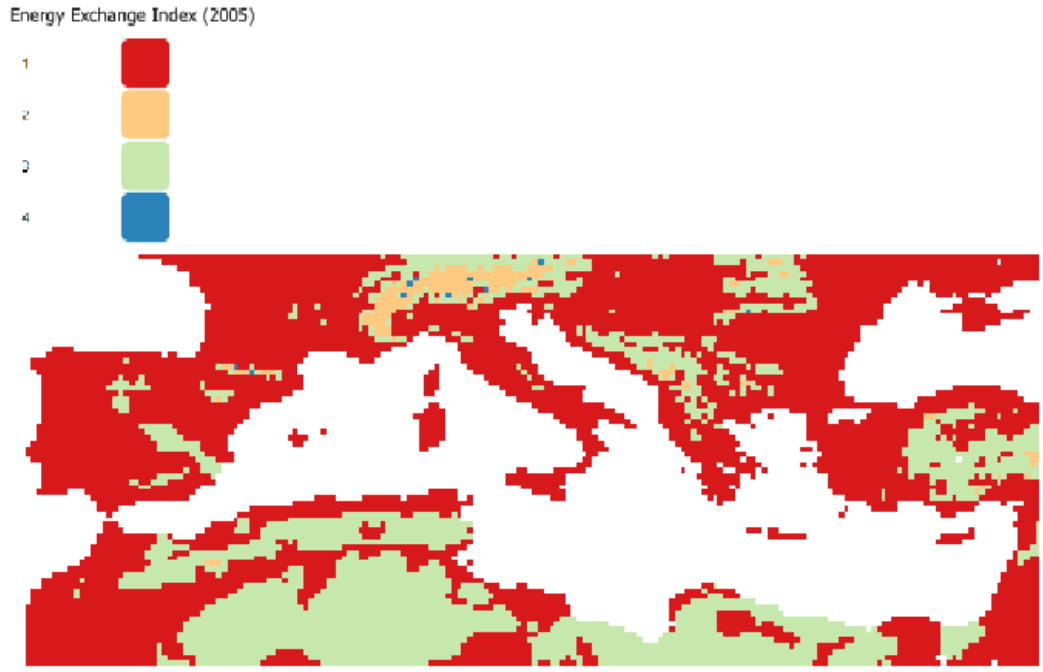

Figure 26: Energy Exchange Index (EEI) spatial distribution in 2005. The four different colored ranges of values represent four sensitivity stages - "very low", "low", "high" and "very high" from the minimum to the maximum range of values.

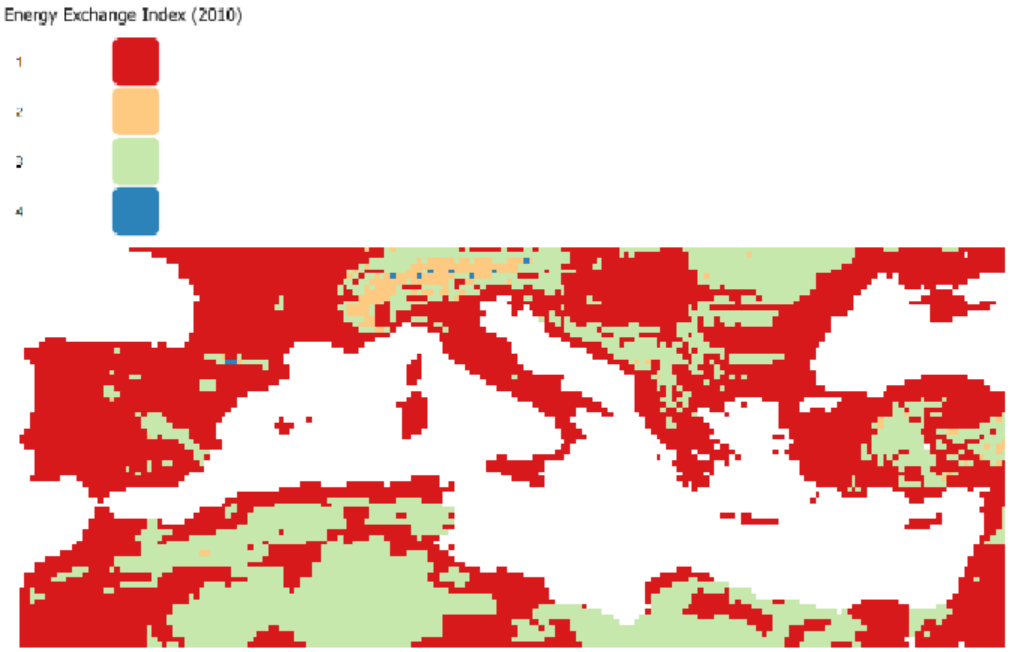

Figure 27: Energy Exchange Index (EEI) spatial distribution in 2010. The four different colored ranges of values represent four sensitivity stages - "very low", "low", "high" and "very high" from the minimum to the maximum range of values.

Figure 28: Energy Exchange Index (EEI) spatial distribution in 2010. The four different colored ranges of values represent four sensitivity stages - "very low", "low", "high" and "very high" from the minimum to the maximum range of values.

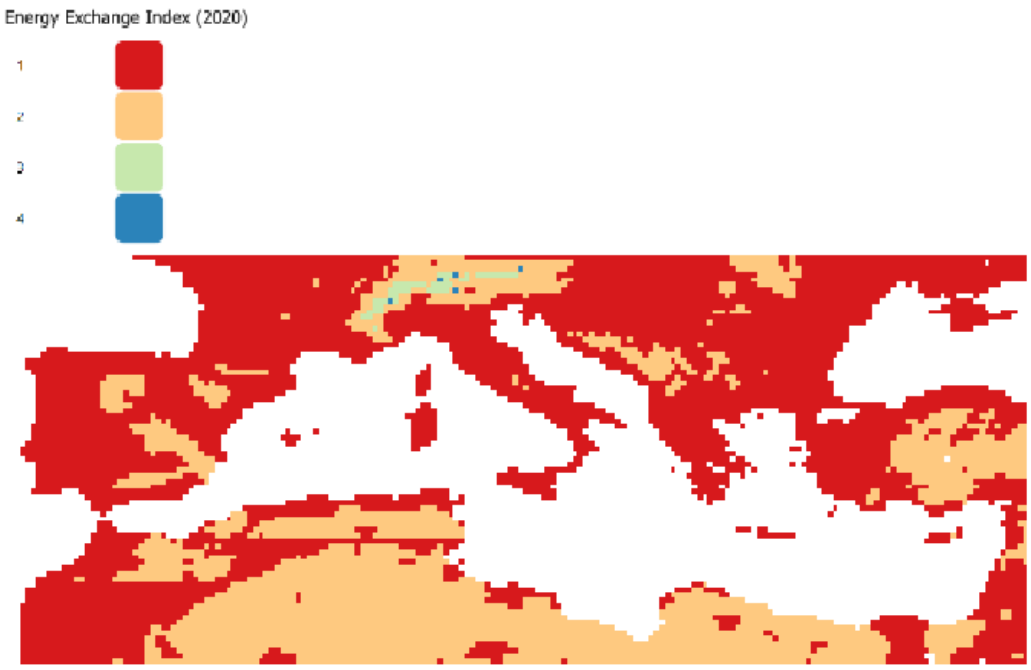

Figure 29: Energy Exchange Index (EEI) spatial distribution in 2020. The four different colored ranges of values represent four sensitivity stages - "very low", "low", "high" and "very high" from the minimum to the maximum range of values.

3.6 Environmental Sensitivity Area Index

The environmental sensitivity of an area to desertification is a consequence of the interaction between indicators pertaining to erosion and desertification phenomena. Indeed, the environmental sensitivity of a given area to desertification is contingent upon several factors, including climate, soil characteristics, vegetation, and topography. By analyzing the characteristics and degree of interaction of the aforementioned factors, it is possible to ascertain the degree of environmental sensitivity of a given area. Furthermore, environmental sensitivity is contingent upon socio-economic factors, as human behavior and social and economic actions can precipitate changes in various environmental characteristics. The calculation of environmental sensitivity scores is performed in two stages from a mathematical perspective. In the initial phase of the analysis, five intermediate quality levels are calculated based on soil, climate, vegetation, land use and energy. In the second stage, the final ESAI is calculated for each area. This method represents an updated iteration of the approach initially developed and evaluated in the MEDALUS III project[22].

The ESAI was calculated using the results of the five indicators previously reported, according to the Equation (2). It can thus be stated that the areas susceptible to soil erosion are

[22] Ferrara Agostino [*et al.*], " ESI – method ", *Identification and assessment of Environmentally Sensitive Areas by Remote Sensing. MEDALUS III 2.6.2. - OU Final Report*, vol. 2, 2004, p. 67-83, accessible by https://esdac.jrc.ec.europa.eu/public_path/shared_folder/projects/DIS4ME/esi_jan_05/method.htm [Consulted 18/05/2024]

distributed throughout the study area, as illustrated in Figures 27-31. Higher values of ESAI indicate area with high sensitivity to soil erosion, while lower values indicate areas with minimal change.

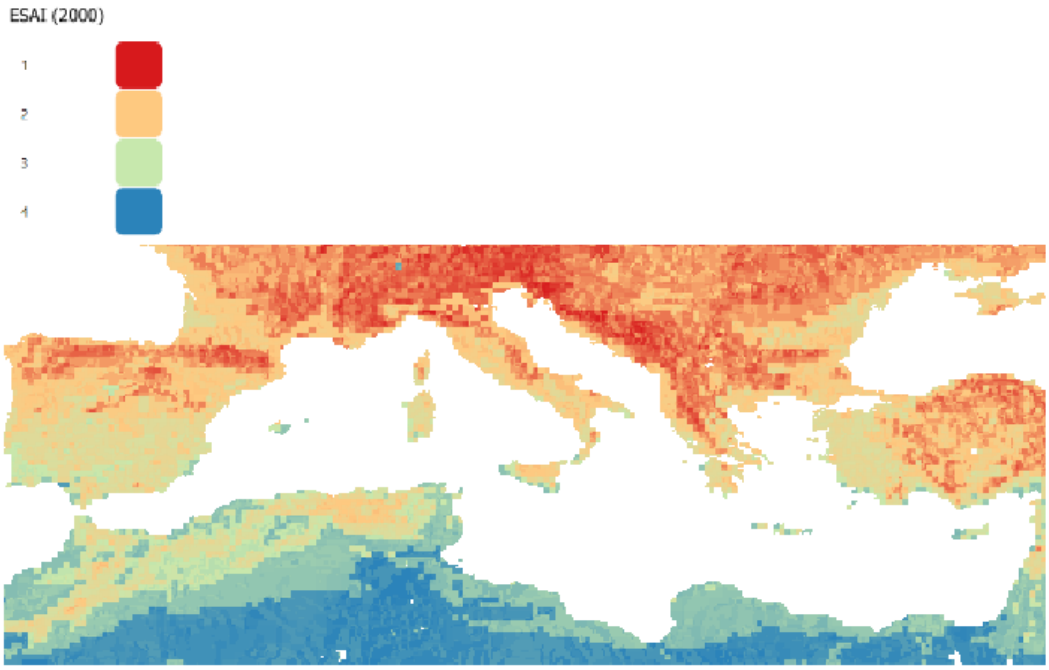

Figure 30: Environmental Sensitivity Area Index (ESAI) spatial distribution in 2000. The four different colored ranges of values represent four sensitivity stages - "very low", "low", "high" and "very high" from the minimum to the maximum range of values.

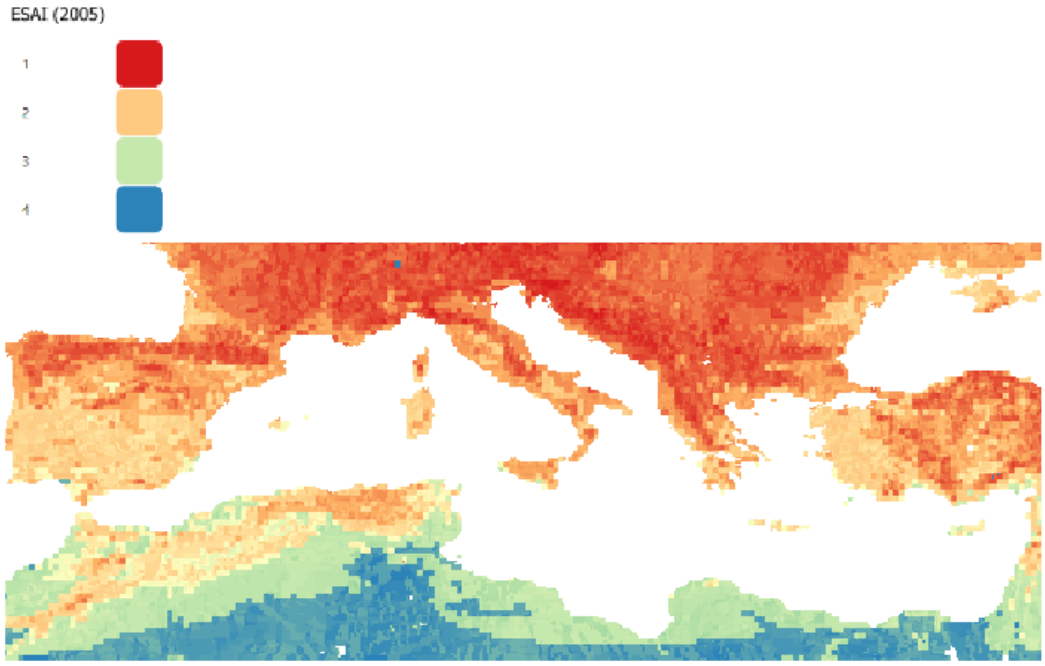

Figure 31: Environmental Sensitivity Area Index (ESAI) spatial distribution in 2005. The four different colored ranges of values represent four sensitivity stages - "very low", "low", "high" and "very high" from the minimum to the maximum range of values.

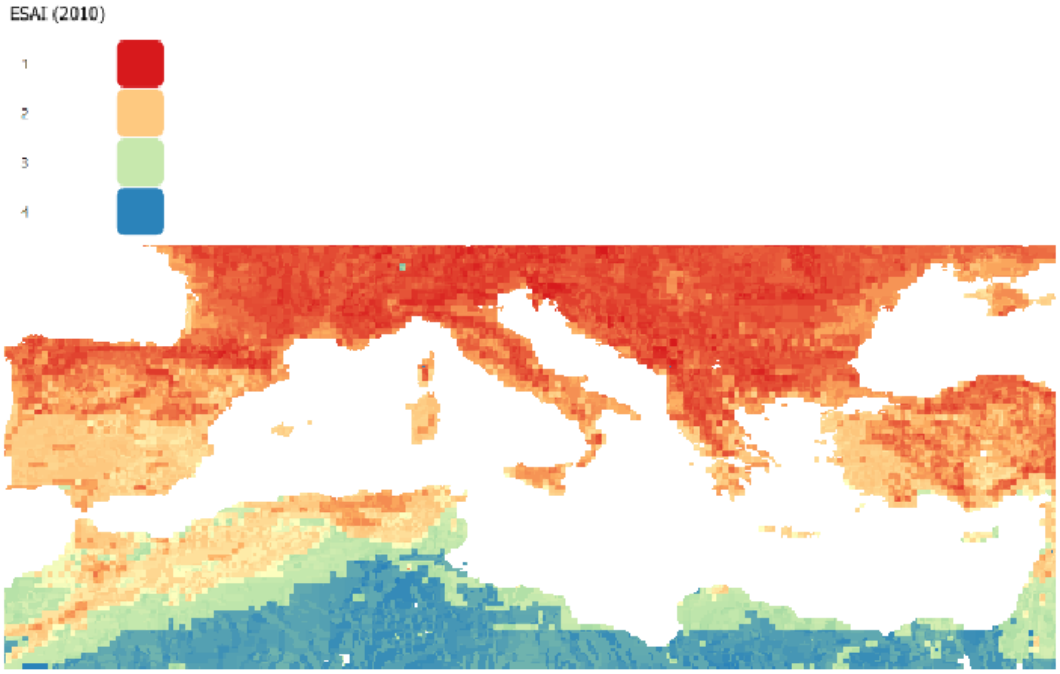

Figure 32: Environmental Sensitivity Area Index (ESAI) spatial distribution in 2010. The four different colored ranges of values represent four sensitivity stages - "very low", "low", "high" and "very high" from the minimum to the maximum range of values.

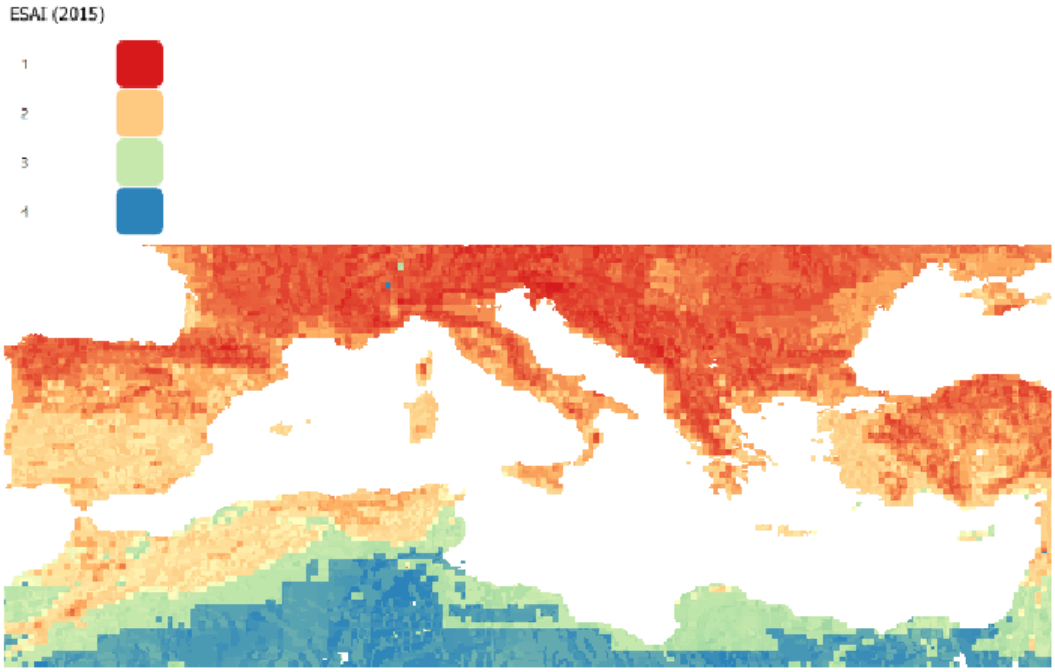

Figure 33: Environmental Sensitivity Area Index (ESAI) spatial distribution in 2015. The four different colored ranges of values represent four sensitivity stages - "very low", "low", "high" and "very high" from the minimum to the maximum range of values.

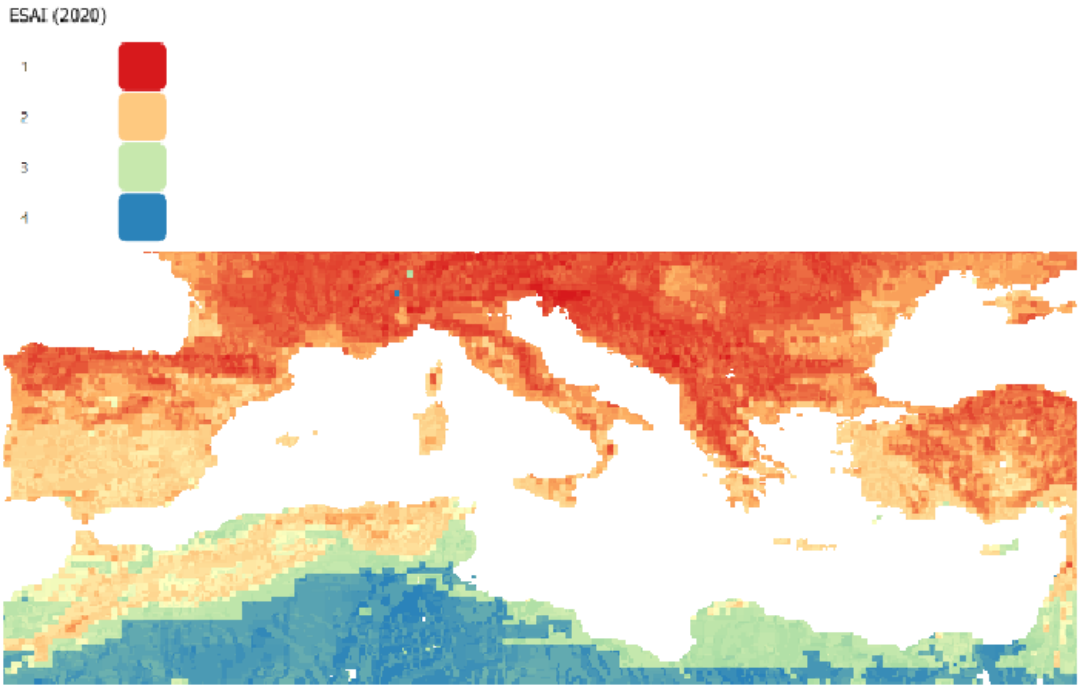

Figure 34: Environmental Sensitivity Area Index (ESAI) spatial distribution in 2020. The four different colored ranges of values represent four sensitivity stages - "very low", "low", "high" and "very high" from the minimum to the maximum range of values.

The ESAI was calculated using the results of the five indices reported previously using Equation (2). It can thus be started that the sensitive areas for soil erosion are scattereded throughout the study area, as illustrated in Figures 27-31. In particular, higher values of ESAI indicate areas with high sensitivity to soil erosion, while lower values indicate areas with greater resilience.

In particular in the year 2000, the Mediterranean countries that appear to exhibit the highest ESAI values (blue and green) and consequently the highest susceptibility to soil erosion are Syria, Lebanon Israel, Palestine, Egypt, Libya, Tunisia, Algeria, Morocco, the southern region of Italy and the western region of Turkey with excedingly high rates observed in the southern part. In 2005 there was a decrease in ESAI values, with the majority of the map displaying red and the vulnerable countries appearing orange. In 2010, there was a decrease in ESAI values in Spain, France, Italy, Malta, Slovenia, Croatia, Bosnia and Herzegovinia, Montenegro, Greece, Albenia and Turkey, while in Syria, Lebanon, Israel, Palestine, Egypt, Libya, Tunisia, Algeria and Morocco prices are increasing, with the exception of the north-easter parts of Morocco and Algeria, where prices remained low. Conversely, in 2015, ESAI prices are increasing for all Mediterranean countries. In 2020 this discrepancy is predominantly evident in the countries in the southern portion of the map. In particular, it was found that from 2000 to 2020 across the Mediterranean, ESAI values have increased, thereby rendering the regions vulnerable to land degradation, with the southern part being the most at risk.

The causes of this degradation can be attributed to human activity, including overpopulation, unbanisation and tourism, which have resulted in the destruction and exploitation of natural resources. The occurrence of extreme weather events has the potential to result in soil erosion, a reduction in precipitation levels which will result in the gradual development of arid conditions and the subsequent desertification of the area in question. The destruction of vast swathes of forest by wildfires, every year the Mediterranean is struck by more than 50.000 fires which burn up to 800.000 hectares of forests[23], the impact of extreme temperatures, the devastation wrought by floods, major coastal floods affecting Mediterranean countries occurred in Italy in 2009, Greece in 2013, Spain in 2015/2016 and Portugal in 2020[24]. and the alteration of an area's geomorphology by earthquakes, On 30 October 2020 a 7.0 Richter earthquake occurred in the eastern Aegean Sea, between the Greek island of Samos and Turkey's Aegean coast[25], contribute to the land degradation.

[23] WWF Mediterranean Program Office, "Forest fires in the Mediterranean", WWF official website, July 2004, p. 1-8, accessible by https://www.wwfmmi.org/?14477/Forest-fires-in-the-Mediterranean [Consulted 06/06/2024]

[24] Ciampa Francesco [*et al.*], "Flood Mitigation in Mediterranean Coastal Regions: Problems, Solutions, and Stakeholder Involvement", *Sustainability,* September 2021, vol. 13, no. 18, p. 10-474. DOI: https://doi.org/10.3390/su131810474 [Consulted 07/06/2024]

[25] Akinci Aybige [*et al*.], "The 30 October 2020, M7.0 Samos Island (Eastern Aegean Sea) Earthquake: effects of source rupture, path and local-site conditions on the observed and simulated ground motions", *Earthquake Engineering,* June 2021, vol. 19, no. 12, p. 4745-4771. DOI: 10.1007/s10518-021-01146-5 [Consulted 07/06/2024]

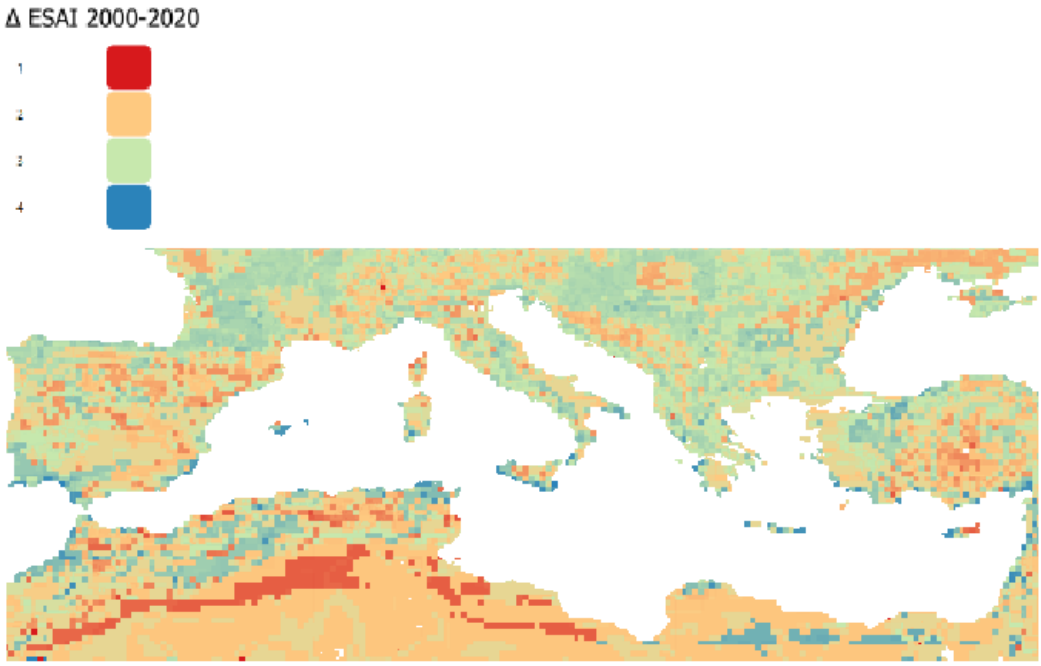

Figure 35:Environmental Sensitivity Area Index (ESAI) spatial distribution in 2000-2020. The four different colored ranges of values represent four sensitivity stages - "very low", "low", "high" and "very high" from the minimum to the maximum range of values.

Comparing the whole considered period from 2000 to 2020 it is observed in figure 35 that many coastal areas in the Mediterranean displayed an increase of ESAI (blue colour), notably south Spain, South Italy, Levant region, Tunisia, and islands such as Majorca, Sicily and Crete. On the contrary inland areas away from the sea (both in Europe and Africa), showed minor changes. Additionally, a lot of mountainous regions in the Mediterranean displayed a decrease of ESAI (red colour), particularly of Algeria, Morocco and Libya, but also seen in Spain and Turkey.

Figure 36:Environmental Sensitivity Area Index (ESAI) spatial distribution in 2000-2005. The four different colored ranges of values represent four sensitivity stages - "very low", "low", "high" and "very high" from the minimum to the maximum range of values.

In figure 36, in Egypt, observed a pattern of red, which may mean that ESAI decreased overall in the region, especially close to the river Nile. Sicily shows a green/blue pattern in the southern shores indicating an ESAI increase, therefore a soil improvement in this period. In the rest of the areas, no major land degradation is observed.

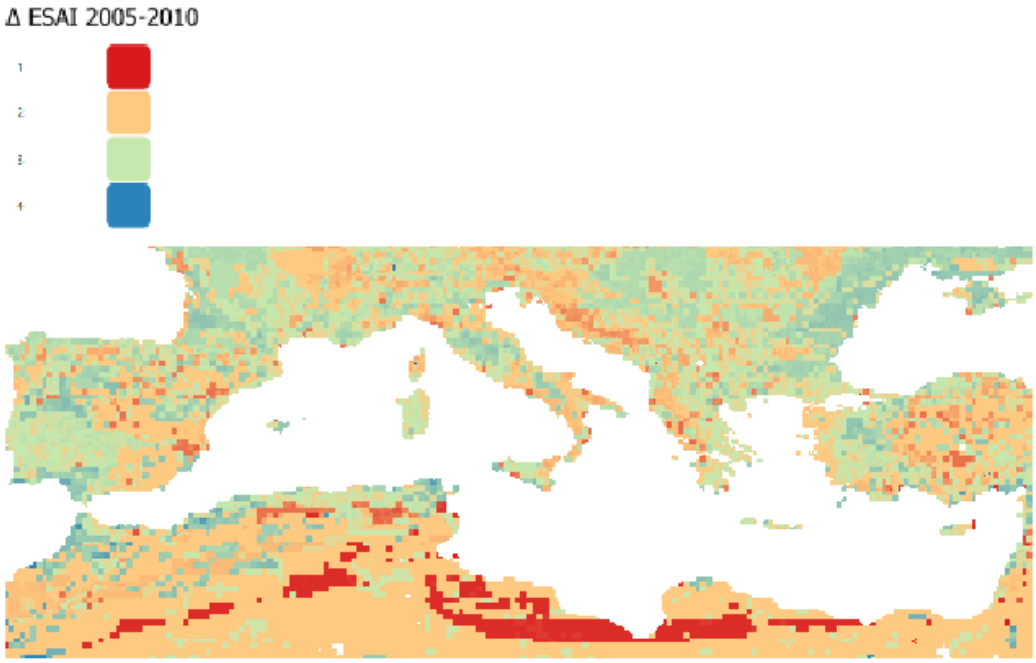

Figure 37:Environmental Sensitivity Area Index (ESAI) spatial distribution in 2005-2010. The four different colored ranges of values represent four sensitivity stages - "very low", "low", "high" and "very high" from the minimum to the maximum range of values.

North Africa areas, from Morocco to Egypt, show a notable decrease in ESAI (red colour) that signifies that the soil became more prone to degradation within this period (2005-2010), as shown in figure 37. European regions show no major changes in ESAI in this period (2005-2010), as there are no clear areas (red or blue) where ESAI changes significantly. Certain areas in Spain, Italy, Greece and Turkey seem to have ESAI decrease (red colour) but these are small and sporadic, and no pattern/conclusion can be drawn.

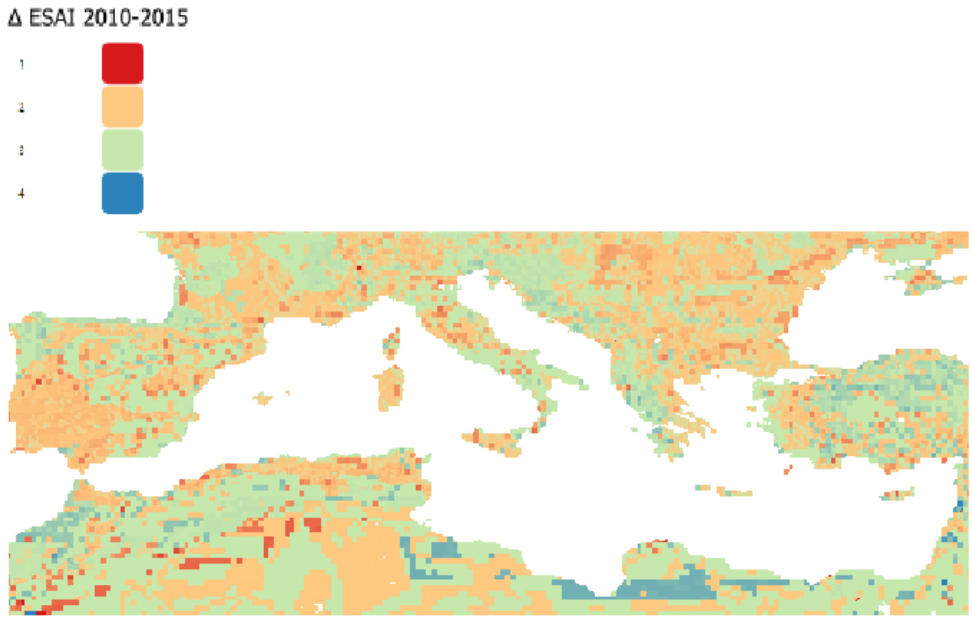

Figure 38:Environmental Sensitivity Area Index (ESAI) spatial distribution in 2015-2010. The four different colored ranges of values represent four sensitivity stages - "very low", "low", "high" and "very high" from the minimum to the maximum range of values.

Overall, no significant changes are observed in ESAI in this period (2010-2015) in figure 38, in both the European and African continents around the Mediterranean. Certain areas in north Africa (Algeria and Morocco) show a decrease in ESAI (red colour), while others (Egypt and Libya) show an increase in ESAI (blue colour) and European regions show no major changes in ESAI in this period (2010-2015), as there are no clear areas (red or blue) where ESAI changes significantly.

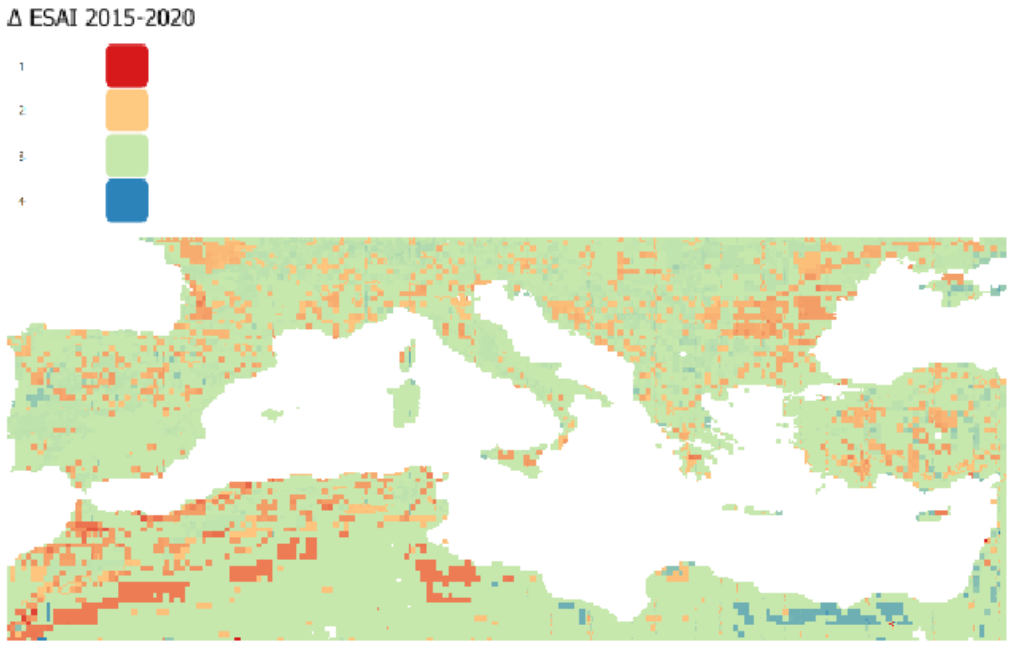

Figure 39:Environmental Sensitivity Area Index (ESAI) spatial distribution in 2015-2020. The four different colored ranges of values represent four sensitivity stages - "very low", "low", "high" and "very high" from the minimum to the maximum range of values.

The ESAI change in this period (figure 39) is very evenly distributed compared to other periods. Similarly with the previous period (2010-2015) some areas in north Africa (Algeria and Morocco) show an decrease in ESAI (red colour), while others (Egypt and Libya) show a increase in ESAI (blue colour), maintaining the previous pattern. Europe in particular shows a very stable ESAI within this period. As well as the coastal regions in the Mediterranean which also show no major changes in ESAI.

It can be concluded that the European countries have significantly lower ESAI values compared to those in North Africa, indicating that the southern Mediterranean is more vulnerable to soil erosion than the northern Mediterranean. Also, coastal areas across the Mediterranean exhibit similar ESAI values as small differentiation observed. As one moves further inland in Europe, ESAI values tend to decrease, whereas in North Africa, they increase. This pattern may be attributed to the differing geomorphology of the two regions, with Europe characterized by more forests and mountainous terrain, while North Africa is dominated by desert landscapes. While there is a significant difference in ESAI values between the northern and southern Mediterranean regions, there is no notable variation between the eastern and western Mediterranean, where the values remain similar. More generally, patterns of ESAI regions (e.g. south blue and north red) remain similar. Probably influenced by the general morphology of different areas.

Overall, ESAI values have decreased compared to 2000. North Africa, particularly Algeria and Tunisia showed notable decrease. France, Italy and the Balkans have also seen substantial decrease. Inland areas (further away from Mediterranean) show less ESAI changes (more stable regions). Europe is observed to have a more stable ESAI (more resistant to changes) compared to Africa over this period of 20 years.

In conclusion, the delta figures 35-39 directly compare ESAI of the same area in 2 different time periods. These figures indicate with 'red' areas where ESAI increased (soil more susceptible to degradation) and 'blue' areas where ESAI decreased (soil became more stable). Thus, the distinction between red and blue areas provides a picture of where soil degradation has worsened or improved, with the aim of mitigating land degradation.

4. CONCLUSIONS

4.1 Discussion

The objective of this thesis is to identify and assess the areas of the Mediterranean that are vulnerable to land degradation using satellite data. This data, once collected, was initially processed to calculate (Equation 2) QI to detect areas of environmental risk affected by the MEDALUS method[26]. Five indicators (CQI, DI, VQI, SQI and EEI) were calculated and analyzed (Tables 1,2,3,4,5, and Figures 2 to 26). The combination of the above indicators leads to the ESAI (Figures 27-31), which provides accurate data on the environmental quality of the Mediterranean.

4.2 Conclusions and Recommendations

The CQI indicates a marked shift in the Mediterranean climate (Figures 5-9), characterized by heightened climate sensitivity, with the northern countries exhibiting the most pronounced changes between 2000 and 2020. The northern Mediterranean countries are characterized by a more favorable climate than their southern counterparts, a phenomenon that can be attributed to a combination of geographical, methodological, and environmental factors. Spain, France, Italy, and Balkan countries have exhibited a decline in CQI values, whereas in the southern Mediterranean, including Egypt, Libya, Tunisia, Algeria and Morocco, there have been considerable fluctuations, resulting in heightened climate sensitivity.

The results presented in the DI (Figures 10-14) indicate a gradual increase in population in urban areas over the period spanning from 2000 to 2020. This observation is particularly evident in countries located in the north-eastern Mediterranean region, as well as in Algeria. In contrast, the southern part of the Mediterranean, which includes countries such as Egypt, Libya, Tunisia, and Morocco, exhibits a lower demographic index with minimal fluctuations over time.

The SQI demonstrates that there are substantial alterations in soil quality in Mediterranean countries at five-year intervals. The SQI shows considerable fluctuations over the 20-year period from 2000 to 2020. These fluctuations indicate heightened soil sensitivity, particularly in the southern countries of the Mediterranean region, rendering them susceptible to land degradation.

The VQI revealed significant alterations in the geographical distribution and quality of vegetation in the Mediterranean between 2000 and 2020 (Figures 17-21). The discrepancy in values between the years 2000 and 2020 is striking, with elevated values in 2020 prevalent across the northern Mediterranean and diminished low values confined to portions of Algeria, Libya, and Greece. This contrasts with the 2000 data, where the areas with high values in the index were more expansive, suggesting a deterioration in the situation.

[26] Ferrara Agostino [*et al*.], " ESI – method ", *Identification and assessment of Environmentally Sensitive Areas by Remote Sensing. MEDALUS III 2.6.2. - OU Final Report*, vol. 2, 2004, p. 67-83, accessible by https://esdac.jrc.ec.europa.eu/public_path/shared_folder/projects/DIS4ME/esi_jan_05/method.htm [Consulted 18/05/2024]

In examining the EEI, a comparison of the years 2000, 2005, 2010, 2015 and 2020 reveals minor fluctuations in the index between 2000 and 2020. Conversely, the years 2005, 2010 and 2015 exhibit elevated EEI values across Algeria, Libya, Egypt, northern Italy, parts of Turkey and Montenegro. This renders these areas particularly susceptible to land degradation.

In consideration of the ESAI, it can be assumed that the areas susceptible to land degradation are distributed throughout the study area, as illustrated in Figures 27-31. Higher ESAI values indicate areas with high susceptibility to soil erosion, while low values suggest areas with minimal changes. In 2000, the Mediterranean countries exhibiting the highest ESAI values and consequently, the greatest susceptibility to soil erosion were Syria, Lebanon, Israel, Palestine, Egypt, Libya, Tunisia, Algeria, Morocco, southern Italy, and western Turkey, with particularly elevated rates observed in the southern regions of these countries. In 2005, there was a general decline in ESAI prices across most of the map. In 2010, there was decrease in ESAI prices in Spain, France, Italy, Malta, Slovenia, Croatia, Bosnia and Herzegovina, Montenegro, Greece, Albania, and Turkey. However, there was an increase in prices in Syria, Lebanon, Israel, Palestine, Egypt, Libya, Tunisia, Algeria, and Morocco, except for the north-easter regions of Morocco and Algeria, where prices remained low. In contrast, the 2015 data indicates an increase in ESAI prices across all Mediterranean countries. In 2020, the disparity is most pronounced in the countries situated in the southern portion of the map. It was found that from 2000 to 2020 across the Mediterranean, ESAI values exhibited a slight, gradual increase. This increase has the effect of rendering the regions sensitive to land degradation, with the southern part being the most at risk.

To summarize, the data used in this study are of high quality and have an appropriate spatial resolution, making them suitable for regional-scale studies. This thesis concentrates on areas in the Mediterranean that are particularly susceptible to degradation, employing the MEDALUS methodology[27] to illustrate this vulnerability. The aim of this is to identify areas within the Mediterranean region that are susceptible to land degradation through the utilization of satellite data. The utilization of this data affords the opportunity to monitor extensive areas with a high degree of precision, which is vital for the effective management of natural resources and the safeguarding of vulnerable regions, in order to pay particular attention to the proper management of natural resources and ecosystems, so as to gradually reduce this phenomenon[28]. The finding of this study can be deemed beneficial for future endeavors, assisting in the safeguarding of environmental sustainability, natural ecosystems, forests, and the quality of life, with the ultimate objective of reducing the vulnerability of Mediterranean land degradation.

[27] Ferrara Agostino [*et al*.], " ESI – method ", *Identification and assessment of Environmentally Sensitive Areas by Remote Sensing. MEDALUS III 2.6.2. - OU Final Report*, vol. 2, 2004, p. 67-83, accessible by https://esdac.jrc.ec.europa.eu/public_path/shared_folder/projects/DIS4ME/esi_jan_05/method.htm [Consulted 18/05/2024]

[28] Bantigegn Sisay, "Natural resource degradation tendencies in Ethiopia: a review", *Environmental Systems Research*, October 2020, vol. 9, no. 1. DOI: 10.1186/s40068-020-00194-1 [Consulted 04/06/2024]

Bibliography

Akinci Aybige [*et al*.], "The 30 October 2020, M7.0 Samos Island (Eastern Aegean Sea) Earthquake: effects of source rupture, path and local-site conditions on the observed and simulated ground motions", *Earthquake Engineering,* June 2021, vol. 19, no. 12, p. 4745-4771.
DOI: 10.1007/s10518-021-01146-5 [Consulted 07/06/2024]

Bantigegn Sisay, "Natural resource degradation tendencies in Ethiopia: a review", *Environmental Systems Research*, October 2020, vol. 9, no. 1.
DOI: 10.1186/s40068-020-00194-1 [Consulted 04/06/2024]

Bolles Dana, "The Effects of Climate Change" in *Climate Change*, NASA official web site, accessible by https://science.nasa.gov/climate-change/effects/ [Consulted 24/07/2024]

Cherif Semia, [*et al*.], "Drivers of Change" in (Ed. Cramer W. *et al.) Climate and Environmental Change in the Mediterranean Basin. First Mediterranean Assessment Report (Mar 1),* Marseille, UNEP/MAP, 2020, p. 59-1034.
DOI: 10.5281/zenodo.7224821 [Consulted 24/07/2024]

Ciampa Francesco [*et al.*], "Flood Mitigation in Mediterranean Coastal Regions: Problems, Solutions, and Stakeholder Involvement", *Sustainability,* September 2021, vol. 13, no. 18, p. 10-474.
DOI: https://doi.org/10.3390/su131810474 [Consulted 07/06/2024]

European Space Agency, " Explore MERIS - Earth Online", *MERIS Applications*, 2022, accessible by https://earth.esa.int/eogateway/instruments/meris [Consulted 09/06/2024]

European Space Agency, " Sentinel-2", *S2 Mission,* accessible by https://sentiwiki.copernicus.eu/web/s2-mission [Consulted 09/05/2024]

FAO, "The State of the World's Forests", in *Forests, biodiversity and people,* Rome, FAO and UNEP, 2020, p. 1-214.
DOI: https://doi.org/10.4060/ca8642en [Consulted 16/05/2024]

Ferrara Agostino [*et al*.], " ESI – method ", *Identification and assessment of Environmentally Sensitive Areas by Remote Sensing. MEDALUS III 2.6.2. - OU Final Report*, vol. 2, 2004, p. 67-83, accessible by https://esdac.jrc.ec.europa.eu/public_path/shared_folder/projects/DIS4ME/esi_jan_05/method.htm [Consulted 18/05/2024]

Huffman George, " Global Precipitation Measurement Mission", *Global Precipitation Measurement,* NASA, 2014, accessible by https://gpm.nasa.gov/missions/GPM [Consulted 01/04/2024]

Kaiser Mohammad Shakil, "Land Degradation: Causes, Impacts, and Interlinks with the Sustainable Development Goals", in (Ed. Walter Leal Filho) *Encyclopedia of the UN Sustainable Development Goals*, Switzerland, Sprinter, 2021, p. 1-13.

DOI: https://doi.org/10.1007/978-3-319-71062-4_48-1 [Consulted 20/06/2024]

Kolios Stavros [*et a*l.], " Detection of areas susceptible to land degradation in Cyprus using remote sensed data and environmental quality indices", *Land Degradation & Development,* vol. 29, no 8, May 2018, p. 2338-2350.
DOI: 10.1002/ldr.3024 [Consulted 26/02/2024]

Kandice L. [*et al.*], "A 29-year time series of annual 300 m resolution plant-functional-type maps for climate models", *Earth Syst. Sci. Data,* vol. 15, May 2023, p.1465 – 1499.
DOI: https://doi.org/10.5194/essd-15-1465-2023 [Consulted 17/03/2024]

Lisetskii F.N. [*et al*.] "Catena linking of landscape-geochemical processes and reconstruction of pedosedimentogenesis," *CATENA*, vol. 28, no. 3-4,2020, p.157-169.
DOI: https://doi.org/10.1016/j.catena.2019.104300 [Consulted 08/04/2024]

Magliulo Paolo, [*et al*.] "Changes in Land-Cover/Land-Use Pattern in the Fortore River Basin (Southern Italy) and Morphodynamic Implications", *Land*, vol. 12, no 7, 2023, p.13-93.
DOI: https://doi.org/10.3390/land12071393 [Consulted 03/05/2024]

Pawson Steven, " MERRA-2 ", *Modern-Era Retrospective analysis for Research and Applications, Version 2*, NASA, September 2022, accessible by https://gmao.gsfc.nasa.gov/reanalysis/MERRA-2/ [Consulted 12/06/2024]

Semion Polivon, "Increased Anthropogenic Activity in the Mediterranean Since the Opening of the Suez Canal", in (Ed. Lutmar C., Rubinovitz Z.) *The Suez Canal: Task Lessons and Features Challenges,* London*,* Palgrave Macmillan, January2023, p.217-229.
DOI: https://doi.org/10.1007/978-3-031-15670-0_11 [Consulted 12/07/2024]

S. Harris, [*et al*.], "Temperate Ecosystems" in (Ed. Burley Jeffery) *Encyclopedia of Forest Sciences*, 2004, Massachusetts, Elsevier, p. 1414-1458, accessible by https://www.sciencedirect.com/referencework/9780121451608/encyclopedia-of-forest-sciences [Consulted 09/04/2024]

Warner Koko, [*et al*], "Climate change, environmental degradation and migration", *Natural Hazards*, vol. 55, no 3, August 2009, p. 689-715.
DOI: https://doi.org/10.1007/s11069-009-9419-7 [Consulted 3/07/2024]

Wulder Michael [*et al*.] "How free data has enabled the science and monitoring promise of Landsat. ", *Remote Sensing of Environment,* July/2012 vol. 122, p. 2-10.
DOI: https://doi.org/10.1016/j.rse.2012.01.010 [Consulted 16/05/2024]

WWF Mediterranean Program Office, "Forest fires in the Mediterranean", WWF official website, July 2004, p. 1-8, accessible by https://www.wwfmmi.org/?14477/Forest-fires-in-the-Mediterranean [Consulted 06/06/2024]

Žiga Malek, [*et al*.],"Global change effects on land management in the Mediterranean region", *Global Environmental Change,* Vol. 50, May 2018, p.238-254.

DOI: https://doi.org/10.1016/j.gloenvcha.2018.04.007 [Consulted 01/04/2024]